Quantum theory of electronic properties in doped semiconductors by an extension of the method of the bent-band theory

Masumi Takeshima
Electronics Research Laboratory, Matsushita Electronics Corporation, Takatsuki, Osaka 569, Japan
(Received 10 August 1988; revised manuscript received 27 February 1989)

A quantum theory for the electronic states in doped semiconductors is given on the basis of the Green's-function formalism by an extension of the bent-band theory. This semiclassical theory neglects all quantum correction terms for the ease of summing up all terms of multisite and multiple Born scatterings and therefore gives a poor explanation of impurity band tails observed in heavily doped semiconductors. The present theory includes quantum correction terms of all orders in a series expansion, and a formally exact solution is obtained for the one-particle Green's function by an extension of the method developed previously for the bent-band model. By picking up dominant terms for practical calculation, it is shown that the present theory gives a better explanation of observed band tails but a worse explanation of observed low-temperature conductivities than the bent-band theory. For obtaining a good explanation of the conductivities, it is assumed that there are localized levels with degeneracy unity at energies below some value. By also taking into account the exchange effect, experimental data of both the density of states and the low-temperature conductivity are shown to be well explained by the present theory.

I. INTRODUCTION

Electrical and optical properties of doped semiconductors are strongly affected by impurity band tails which appear as a result of the impurity doping. The low-temperature conductivity in a heavily doped semiconductor is a typical example and is of academic interest because electrons interact strongly with many impurities simultaneously, as in the localization and declocalization problem. Various theories[1-7] have been developed so far in order to understand the conduction in the presence of ionized impurities. Although the theories have turned out to be useful[8,9] at high temperatures and/or light doping levels, they cannot explain[10] the conduction at heavy doping levels, especially at low temperatures. By even more careful calculations,[11-13] the experimental dependence of the low-temperature conductivity on the doping level has not been satisfactorily explained. The reason may be that the above calculations have been performed neglecting important effects of the band tails, of the simultaneous interaction of each electron with many impurities, and of the Born scatterings of higher than second order.

As for the impurity band tails, there have been a number of calculations, starting with earlier calculations[14-16] based on perturbation and propagator techniques. These calculations have led to band tails which are cut off too sharply. Kane[17] has calculated the density of states (DOS) with the use of the Thomas-Fermi approach for the fluctuating potential, obtaining a Gaussian tail. This is a disadvantage because simple exponential tails are often observed from experiments.[18,19] As a quantum counterpart of the semiclassical theory of Kane, Halperin and Lax[20] have offered a minimum counting method which is rigorous only for sufficiently deep states. Sayakanit and Glyde[21] have improved the method with the use of the variational principle but the theory has been found[22,23] to give a poor description of experiments.

On the other hand, a semiclassical approach has been adopted by Bonch-Bruevich[24] with the use of the bent-band model (BB), which is useful for the potential varying slowly enough. Instead of solving directly the differential equation as was done by Bonch-Bruevich, the present author has reached the same result[25] with the the use of the diagram method, taking into account all terms of multisite and multiple Born scatterings. With the use of the one-particle Green's function obtained in this way, the Auger recombination rate and the low-temperature conductivity have been calculated. Despite the agreement found[25-27] between the calculations and experiments, it has also been found[22,23,25] that the BB theory gives values of the DOS much smaller than experimental ones especially in the band-tail region. This directly reflects the fact that a semiclassical approach of the BB theory is not applicable especially at low energies, because the BB model is useful under a sufficiently slow spatial variation of the impurity potential at least in an effective sense. Therefore, the agreement between the theory and experiments on the electronic properties does not have a solid basis.

A cure has been provided by the present author,[22,23] who has devised a semiempirical pseudopotential (SP) approach. In this theory, the BB theory is modified so as to take into account the quantum effect with the use of a semiempirical effective potential. It has turned out that the theory gives a better explanation of the band tails observed experimentally. However, a disadvantage is that we have no solid basis supporting the SP approach. Thus it seems that we still have no theory which satisfactorily gives a quantitative explanation of electronic properties of doped semiconductors in a coherent way.

Recently, the present author has shown[28] that the

two-particle Green's function is, within the framework of the BB model, exactly obtainable with the use of the diagram method. Thus we have both the one-particle Green's function and the two-particle Green's function, so that the conductivity can be calculated more rigorously in this case than in the previous case of the BB theory.[25] It has been found[28,29] that experimental data of the low-temperature conductivity in Si and Ge are considerably well explained by the BB theory at doping levels above the metal-insulator transition. For the calculation, the two-particle Green's function is rewritten as a sum of the free part and the vertex part. The free part, which is given in terms of the one-particle Green's function, has been found to be a key factor determining the conductivity at heavy doping levels. However, experimentally observed band tails are still inexplicable by the BB theory. From this view point, therefore, there is a strong need for a quantum-theoretical treatment as an alternative to the BB model which provides a solid basis for the one-particle Green's function.

The purpose of the present paper is to present a quantum theory giving a rigorous calculation of the one-particle Green's function. Here we take into account the quantum correction terms which have been neglected in the BB theory. Thus we go beyond the BB theory in a direct way. The calculation is done by an extension of the method developed[28] for obtaining the two-particle Green's function in the BB theory. All the terms representing multisite and multiple Born scatterings are summed up and a formal exact solution is obtained in a series. Then a practical form of the solution is given by picking up dominant terms in the series. With the use of the one-particle Green's function obtained, the DOS is calculated. The low-temperature conductivity is calculated from the free part and the vertex part of the two-particle Green's function. The free part is given in terms of the one-particle Green's function obtained by the quantum theory. On the other hand, the vertex part, whose contribution is not very important in the doping range except in the close vicinity of the metal-insulator transition, is given simply by the BB theory.

The quantum theory gives a stronger effect of the impurity doping than the BB theory, leading to larger DOS's in the band-tail region and to shorter relaxation time of carriers. As a result, the conductivities are smaller in the quantum theory than in the BB theory. On the other hand, the BB theory gives much smaller DOS's in the band-tail region and somewhat smaller conductivities than the respective experimental ones. Therefore, the quantum theory gives a better description of the DOS than the BB theory, while the former gives a much worse description of the conductivity than the latter. For this difficulty a cure is provided by assuming that we have localized states at energies below some critical value and that each localized state can be occupied by only a single electron irrespective of the spin multiplicity and the valley number. We consider also various terms due to the electron-electron repulsion via the Coulomb interaction and the electron-electron attraction via the electron-phonon interaction. It is shown that the above assumption of the occupation is especially important in explaining experimental data of the conductivity.

This paper is organized as follows. In Sec. II, a formally exact solution for the one-particle Green's function under the quantum model is given, together with a more tractable but approximate form of the function. These functions are derived in Appendixes A and B. In Sec. III, a practical method for calculating the DOS and the conductivity is described. In Sec. IV, calculated results of the DOS and the conductivity are shown and discussed especially in relation to a new assumption adopted.

II. DERIVATION OF THE GREEN'S FUNCTION

First we present a model for the analysis of the electron-impurity interaction together with a general principle for the calculation. Let us consider the Hamiltonian as a sum of those for the unperturbed-band electrons, the electron-impurity interaction, the electron-electron interaction, and the electron-phonon interaction, details of which are found elsewhere.[28,30] Starting with bare interactions, we obtain screened interactions by the many-body theoretical treatment. Based on these interactions we go into the discussion of the retarded one-particle Green's function $G^R(l\mathbf{k},l\mathbf{k}';\omega)$, where l is the band index, $\mathbf{k}$ and $\mathbf{k}'$ the wave vectors, and ω the energy parameter. Two wave vectors $\mathbf{k}$ and $\mathbf{k}'$ appear in the presence of randomly distributed impurities, and a single band index l appears as a result of neglecting the interband scattering.

Let us consider the impurity potential $\Gamma(\mathbf{r})$ given by

$$\Gamma(\mathbf{r})=\sum_{n=1}^{N_i} U_i(\mathbf{r}-\mathbf{R}_n)\ , \tag{2.1}$$

where N_i is the number of the impurities assumed to be of a single species and $U_i(\mathbf{r}-\mathbf{R}_n)$ is a screened potential due to an impurity at $\mathbf{R}_n$. With the use of the Fourier expansion

$$\Gamma(\mathbf{r})=\sum_{\mathbf{q}} \bar{\Gamma}(\mathbf{q})\exp(j\mathbf{q}\cdot\mathbf{r})\ , \tag{2.2}$$

we obtain[31]

$$G^R(l\mathbf{k},l\mathbf{k}';\omega)=G_0^R(l\mathbf{k},\omega)\left\{\Delta(\mathbf{k}-\mathbf{k}')+\sum_{n=1}^{\infty}\sum_{\mathbf{q}_1\mathbf{q}_2\cdots\mathbf{q}_n}\prod_{m=1}^{n}\left[G_0^R\left[l\mathbf{k}-\sum_{\alpha=1}^{m}\mathbf{q}_\alpha;\omega\right]\bar{\Gamma}(\mathbf{q}_m)\right]\Delta\left[\sum_{m=1}^{n}\mathbf{q}_m-\mathbf{k}+\mathbf{k}'\right]\right\}\ , \tag{2.3}$$

where $\Delta(x)$ is defined as $\Delta(x)=1$ if $x=0$ and $\Delta(x)=0$ otherwise with x as a scalar or a vector; $G_0^R(l\mathbf{k},\omega)$ is the free-particle Green's function

$$G_0^R(l\mathbf{k},\omega)=\frac{1}{\omega-E_l(\mathbf{k})+j0^+} \tag{2.4}$$

with $E_l(\mathbf{k})$ as the unperturbed band energy. Let us suppress l and ω in G^R, G_0^R, and E_l hereafter. With the use of Eq. (2.2), Eq. (2.3) is rewritten as

$$G^R(\mathbf{k},\mathbf{k}')=G_0^R(\mathbf{k})\frac{1}{V}\int d\mathbf{r}\exp[-j(\mathbf{k}-\mathbf{k}')\cdot\mathbf{r}]\sum_{n=0}^{\infty}[G_0^R(\mathbf{k}+j\nabla)\Gamma(\mathbf{r})]^n , \tag{2.5}$$

where $\nabla=\partial/\partial\mathbf{r}$ and V is the crystal volume. A symbolic expression for Eq. (2.5) is

$$G^R(\mathbf{k},\mathbf{k}')=G_0^R(\mathbf{k})\frac{1}{V}\int d\mathbf{r}\exp[-j(\mathbf{k}-\mathbf{k}')\cdot\mathbf{r}]\times\frac{\omega-E(\mathbf{k}+j\nabla)+j0^+}{\omega-E(\mathbf{k}+j\nabla)-\Gamma(\mathbf{r})+j0^+} . \tag{2.6}$$

Because $G^R(\mathbf{k},\mathbf{k}')$ depends on the impurity sites $\mathbf{R}_n$'s through $\Gamma(\mathbf{r})$, we take an ensemble average[24,31] of $G^R(\mathbf{k},\mathbf{k}')$ over the impurity sites, which is defined as

$$\langle G^R(\mathbf{k},\mathbf{k}')\rangle=V^{-N_i}\int d\mathbf{R}_1 d\mathbf{R}_2\cdots d\mathbf{R}_{N_i}G^R(\mathbf{k},\mathbf{k}') =G^R(\mathbf{k})\Delta(\mathbf{k}-\mathbf{k}') . \tag{2.7}$$

The last step of this equation comes from the fact that the space uniformity, which is lost under random distribution of the impurities giving $\mathbf{k}\neq\mathbf{k}'$, is restored under the average distribution giving the momentum conservation $\mathbf{k}=\mathbf{k}'$. $G^R(\mathbf{k})$ is the retarded Green's function in the average impurity distribution, for which the rule of the diagram method is known[31]. Owing to $\mathbf{k}=\mathbf{k}'$ in Eq. (2.7), we have

$$\langle G^R(\mathbf{k},\mathbf{k}')\rangle=\frac{1}{V}\int d\mathbf{r}\exp[-j(\mathbf{k}-\mathbf{k}')\cdot\mathbf{r}]\times\left\langle\frac{1}{\omega-E(\mathbf{k}+j\nabla)-\Gamma(\mathbf{r})+j0^+}\right\rangle . \tag{2.8}$$

In view of this relation, we write $G^R(\mathbf{k},\mathbf{k}')$ as equal to the right-hand side of Eq. (2.8) without average notation hereafter.

Defining the operator

$$O_k(\nabla)=E(\mathbf{k}+j\nabla)-E(\mathbf{k}) , \tag{2.9}$$

$G^R(\mathbf{k},\mathbf{k}')$ is rewritten as

$$G^R(\mathbf{k},\mathbf{k}')=G_0^R(\mathbf{k})\frac{1}{V}\int d\mathbf{r}\exp[-j(\mathbf{k}-\mathbf{k}')\cdot\mathbf{r}]\times\frac{1}{1-G_0^R\Gamma-G_0^RO_k} , \tag{2.10}$$

where $G_0^R\Gamma$ and $G_0^RO_k$ are the abbreviations of $G_0^R(\mathbf{k})\Gamma(\mathbf{r})$ and $G_0^R(\mathbf{k})O_k(\nabla)$. With the use of the expansion

$$\frac{1}{1-G_0^R\Gamma-G_0^RO_k}=\frac{1}{1-G_0^R\Gamma}\sum_{n=0}^{\infty}\left[G_0^RO_k\frac{1}{1-G_0^R\Gamma}\right]^n \tag{2.11}$$

we write $G^R(\mathbf{k},\mathbf{k}')$ as

$$G^R(\mathbf{k},\mathbf{k}')=\sum_{n=0}^{\infty}K_n(\mathbf{k},\mathbf{k}') , \tag{2.12}$$

where

$$K_n(\mathbf{k},\mathbf{k}')=G_0^R(\mathbf{k})\frac{1}{V}\int d\mathbf{r}\exp[-j(\mathbf{k}-\mathbf{k}')\cdot\mathbf{r}]\times\frac{1}{1-G_0^R\Gamma}\left[G_0^RO_k\frac{1}{1-G_0^R\Gamma}\right]^n . \tag{2.13}$$

It should be noted that the term of $n=0$ contains no spatial derivative. The special case where we neglect the terms of $n\geq 1$ and retain only the term of $n=0$ gives the BB approach which is useful for the impurity potential varying slowly enough. The calculations of the one-particle and the two-particle Green's functions based on the BB model have been given previously[28] as a semiclassical approach. In the quantum theory we include now all the terms of $n\geq 1$.

The average Green's function can be given from Eq. (2.12) in the form

$$G^R(\mathbf{k})=\sum_{n=0}^{\infty}K_n(\mathbf{k}) , \tag{2.14}$$

where $K_n(\mathbf{k})$ is defined through an ensemble average of $K_n(\mathbf{k},\mathbf{k}')$ as

$$\langle K_n(\mathbf{k},\mathbf{k}')\rangle=K_n(\mathbf{k})\Delta(\mathbf{k}-\mathbf{k}') . \tag{2.15}$$

Especially $K_0(\mathbf{k})$ is the Green's function in the BB model given[28] by

$$K_0(\mathbf{k})=\frac{1}{j}\int_0^{\infty}ds\exp\left[\frac{js}{G_0^R(\mathbf{k})}+n_i\int d\mathbf{r}\{\exp[-jsU_i(\mathbf{r})]-1\}\right] , \tag{2.16}$$

where n_i is the impurity concentration N_i/V. By an extension of the BB theory[28] for the two-particle Green's function as shown in Appendix A, $K_n(\mathbf{k})$ for $n\geq 1$ is given by

$$K_n(\mathbf{k})=j^{-n-1}\int_0^{\infty}ds_0\exp\left[\frac{js_0}{G_0^R(\mathbf{k})}\right]\int d\mathbf{r}_0\delta(\mathbf{r}_0)\prod_{m=1}^{n}\left[\int_0^{\infty}ds_m\exp\left[\frac{js_m}{G_0^R(\mathbf{k})}\right]\right]\prod_{m=1}^{n}\left[\int d\mathbf{r}_m\delta(\mathbf{r}_m)O_k\left[\sum_{l=m}^{n}\nabla_l\right]\right] \times\exp\left\{n_i\int d\mathbf{r}\left[\exp\left[-j\sum_{m=0}^{n}U_i(\mathbf{r}+\mathbf{r}_m)s_m\right]-1\right]\right\} , \tag{2.17}$$

where $\nabla_l = \partial/\partial r_l$ and $O_p(\sum_{l=m}^{n} \nabla_l)$ should be placed from the left to the right in the increasing order of m. Thus Eq. (2.14) under Eqs. (2.16) and (2.17) offers a formally exact solution for the one-particle Green's function describing the electron-impurity interactive states. Into those equations, other interaction effects are incorporated by replacing $G_0^R(\mathbf{k})$ in Eqs. (2.16) and (2.17) with $G_1^R(\mathbf{k})$ given by

$$G_1^R(\mathbf{k}) = \frac{1}{\omega - E(\mathbf{k}) - \Sigma^R(\mathbf{k})} , \tag{2.18}$$

where $\Sigma^R(\mathbf{k})$ is the self-energy due to those interactions, e.g., the electorn-electron interaction and the electron-phonon interaction.

Let us find a practical formula for $G^R(\mathbf{k})$ from Eqs. (2.14), (2.16), and (2.17) by assuming spherical symmetry of $U_i(\mathbf{r})$ [$\equiv U_i(r)$] and the unperturbed band energy of the form

$$E(\mathbf{k}) = \frac{\hbar^2}{2}\left[\frac{1}{m_\perp}(k_x^2 + k_y^2) + \frac{1}{m_\parallel} k_z^2\right] \tag{2.19}$$

given in terms of the transverse mass $m_\perp$ and the longitudinal mass $m_\parallel$; hereafter ω and $E(\mathbf{k})$ are measured from the unperturbed band edge, $\hbar$ the Planck constant divided by 2π, and $\mathbf{k} = (k_x, k_y, k_z)$. Then the density-of-states mass m_D, the conductivity mass m_C, and an averaged mass m_F are defined by $m_D = (m_\perp^2 m_\parallel)^{1/3}$, $m_C^{-1} = (2m_\perp^{-1} + m_\parallel^{-1})/3$, and $m_F^{-1} = (2m_\perp^{-1/2} + m_\parallel^{-1/2})/(3m_D^{1/2})$, respectively. It is convenient to define also $\mathbf{k}' = (k_x', k_y', k_z')$ under $k_x' = (m_D/m_\perp)^{1/2} k_x$, $k_y' = (m_D/m_\perp)^{1/2} k_y$, and $k_z' = (m_D/m_\parallel)^{1/2} k_z$. All the functions of $\mathbf{k}$ which have been considered hitherto are expressed as the functions of $\mathbf{k}'$; for example, $G^R(\mathbf{k})$ is rewritten as $G^R(\mathbf{k}')$. Noting the relations $\int d\mathbf{k} = \int d\mathbf{k}'$ and

$$E(\mathbf{k}) = \frac{\hbar^2}{2m_D}|\mathbf{k}'|^2 \equiv E_D(\mathbf{k}') , \tag{2.20}$$

we then rewrite $\mathbf{k}'$ simply as $\mathbf{k}$ hereafter. Now by summing up dominant terms under approximations as shown in Appendix B, we obtain

$$G^R(\mathbf{k}) = \frac{1}{j}\int_0^\infty dt \exp\left[\frac{jt}{G_1^R(\mathbf{k})} + h(t)\right] , \tag{2.21}$$

where

$$h(t) = n_i \int d\mathbf{r}\left[\exp\left[-jtU_i(\mathbf{r}) - j\frac{t^3}{3}\frac{\hbar^2}{2m_C}|\nabla U_i(r)|^2 + \frac{t^2}{2}\frac{\hbar^2}{2m_C}\nabla^2 U_i(r) - jt^2\frac{\hbar^2}{2m_F}\mathbf{k}\cdot\nabla U_i(r)\right] - 1\right] . \tag{2.22}$$

As pointed out, $\mathbf{k}$ in Eqs. (2.21) and (2.22) is used as $\mathbf{k}'$. It is seen that in the classical limit of $m_C \to \infty$ and $m_F \to \infty$ we have $G^R(\mathbf{k})$ in the BB model.

III. PRACTICAL METHOD FOR CALCULATION

A practical method for calculating the DOS and the conductivity is given considering various interactions under the Thomas-Fermi screening. Assuming singly ionized impurities of one species, we obtain

$$U_i(\mathbf{r}) = -\frac{e^2}{\epsilon_0 r}\exp(-\lambda r) , \tag{3.1}$$

where e is the electronic charge, ϵ_0 the static dielectric constants due to the host lattice, and λ the inverse screening length. The interaction between electrons at $\mathbf{r}_1$ and $\mathbf{r}_2$ is given by $U(\mathbf{r}_1 - \mathbf{r}_2) = -U_i(\mathbf{r}_1 - \mathbf{r}_2)$. As the self-energy in Eq. (2.18) we first consider only the Coulomb term of the lowest order in the screened electron-electron interaction. We have

$$\Sigma_c^R = n_i \int d\mathbf{r}\, U(\mathbf{r}) . \tag{3.2}$$

Then the practical formulas for computing the one-particle Green's function are given by

$$G^R(\mathbf{k},\omega) = \bar{G}^R(\Omega, k)/E_\lambda \tag{3.3}$$

$$\bar{G}^R(\Omega, k) = \frac{1}{j}\int_0^\infty d\xi \exp[j\xi\Omega + \gamma g_1(\xi, k)] , \tag{3.4}$$

$$g_1(\xi, k) = -j\xi + \int_0^\infty dx\, x^2\{H(x,k)\exp[F(x)] - 1\} , \tag{3.5}$$

$$F(x) = j\frac{\xi}{x}\exp(-x) - j\frac{a_c\lambda\xi^3}{6}\left[\frac{1+x}{x^2}\exp(-x)\right]^2 - \frac{a_c\lambda\xi^2}{4}\frac{1}{x}\exp(-x) , \tag{3.6}$$

$$H(k,x) = \left[\sin\left[\tfrac{1}{2}a_F k\xi^2\frac{1+x}{x^2}\exp(-x)\right]\right] \Big/ \left[\tfrac{1}{2}a_F k\xi^2\frac{1+x}{x^2}\exp(-x)\right] , \tag{3.7}$$

$$\Omega = [\omega - E_D(\mathbf{k}) - \Sigma_r^R(\mathbf{k},\omega)]/E_\lambda , \tag{3.8}$$

where $\gamma=4\pi n_i/\lambda^3$, $E_\lambda=e^2\lambda/\epsilon_0$, $a_C=\hbar^2\epsilon_0/(m_Ce^2)$, $a_F=\hbar^2\epsilon_0/(m_Fe^2)$, and $\Sigma_r^R(\mathbf{k},\omega)=\Sigma^R(\mathbf{k},\omega)-\Sigma_C^R$.

For the calculation of the DOS, $\rho(\omega)$ and the conductivity σ, we consider a multivalley semiconductor with the number of the valley ν and the temperature 0 K. For convenience in a later discussion, we assume a general case where the degeneracy is a function of the energy ω given by $f(\omega)$. In the usual method for calculations, the degeneracy due to the spin multiplicity 2 and to the number of the valley ν is given by $f(\omega)=2\nu$. Thus we replace 2ν appearing in the usual expressions as for the DOS, the conductivity, and the inverse screening length with $f(\omega)$. First the DOS and the inverse screening length are determined from[28]

$$\rho(\omega)=-\frac{1}{\pi(2\pi)^3}f(\omega)\int d\mathbf{k}\,\mathrm{Im}G^R(\mathbf{k},\omega) \tag{3.9}$$

and

$$\lambda^2=\frac{4e^2}{\epsilon_0(2\pi)^3}\int d\mathbf{k}\int_{-\infty}^{\omega_F}d\omega\, f(\omega)\mathrm{Im}[G^R(\mathbf{k},\omega)]^2\ . \tag{3.10}$$

Here, ω_F is the Fermi level determined from

$$\int_{-\infty}^{\omega_F}d\omega\,\rho(\omega)=n_i\ . \tag{3.11}$$

Actually, λ^2 is given as a sum of the free part and the vertex part[28] and Eq. (3.10) has been obtained by neglecting the vertex part. Because $G^R(\mathbf{k},\omega)$ depends on λ, Eqs. (3.9)–(3.11) are solved for λ.

The conductivity is given as a sum of the free part σ_1 and the vertex part σ_2, i.e., $\sigma=\sigma_1+\sigma_2$; each part comes from the respective part of the two-particle Green's function. By modification of the expression in Ref. 28, we have

$$\sigma_1=\frac{2e^2\hbar}{3\pi(2\pi)^3m_C}f(\omega_F)\int d\mathbf{k}\,E_D(\mathbf{k})\times[\mathrm{Im}G^R(\mathbf{k},\omega_F)]^2 \tag{3.12}$$

for a cubic crystal. In order to calculate σ_2 we need the two-particle Green's function in the quantum theory, which is not available in the present paper. Therefore we use the expression for σ_2 in the BB theory[28] in view of the finding[28] that the contribution of σ_2 to σ is not very important in the range except in the close vicinity of the metal-insulator transition. We have

$$\sigma_2=\frac{\lambda e^2m_D}{12\pi^3\hbar m_C}f(\omega_F)\int_0^{x_c}dx\int_{-\infty}^{\Omega_F}d\Omega[\mathrm{Im}\bar{G}^R(\Omega,\beta_c;x)-\mathrm{Im}\bar{G}^R(\Omega,\beta_c;\infty)]\times\left\{\frac{2}{x^2}\left[1-\cos\left[\frac{2k}{\lambda}x\right]\right]-\frac{4k}{x\lambda}\sin\left[2\frac{k}{\lambda}x\right]+\frac{2k^2}{\lambda^2}\left[1+\cos\left[\frac{2k}{\lambda}x\right]\right]\right\}. \tag{3.13}$$

Here β_c is some large quantity of the order of 10 (we use $\beta_c=30$ in this paper), $\Omega_F=\omega_F/E_\lambda$, $k=(2\lambda/a_D)(\Omega_F-\Omega)^{1/2}$, and

$$\bar{G}^R(\Omega,\beta_c;x)=\frac{1}{j}\int_0^\infty d\zeta\exp[j\zeta\Omega+\gamma\phi(\zeta,\beta_c;x)]\ , \tag{3.14}$$

where

$$\phi(\zeta,\beta_c;x)=-j\zeta+\frac{1}{4\pi}\int d\mathbf{x}'\left[\exp\left[j\frac{\zeta+\beta_c}{2|\mathbf{x}'-\frac{1}{2}\mathbf{x}|}\exp(-|\mathbf{x}'-\tfrac{1}{2}\mathbf{x}|)+j\frac{\zeta-\beta_c}{2|\mathbf{x}'+\frac{1}{2}\mathbf{x}|}\exp(-|\mathbf{x}'+\tfrac{1}{2}\mathbf{x}|)\right]-1\right]\ , \tag{3.15}$$

$\mathbf{x}'$ and $\mathbf{x}$ are the three-dimensional dimensionless vectors. In Eq. (3.13), x_c is defined as a quantity large enough for $\mathrm{Im}\bar{G}^R(\Omega,\beta_c;x_c)$ to be practically the same as $\mathrm{Im}\bar{G}^R(\Omega,\beta_c;\infty)$. Note that we have

$$\phi(\zeta,\beta_c;\infty)=g\left[\frac{\zeta+\beta_c}{2}\right]+g\left[\frac{\zeta-\beta_c}{2}\right] \tag{3.16}$$

with

$$g(\xi)=-j\xi+\int_0^\infty dx\,x^2\left[\exp\left[j\frac{\xi}{x}\exp(-x)\right]-1\right]\ . \tag{3.17}$$

Now we consider the electron-electron interaction, $\bar{U}_T(\mathbf{q},\omega)$ ($\mathbf{q}$ is the wave vector), as a sum of the Coulomb repulsion and the attraction due to the electron-phonon interaction. We have[30]

$$\bar{U}_T(\mathbf{q},\omega)=\bar{U}(\mathbf{q},\omega)+\zeta(\mathbf{q},\omega)D_0(\mathbf{q},\omega)\ , \tag{3.18}$$

where

$$\bar{U}_T(\mathbf{q},\omega)=\frac{\bar{U}_0(\mathbf{q})}{\epsilon_T(\mathbf{q},\omega)}\ , \tag{3.19}$$

$$\zeta(\mathbf{q},\omega)=\frac{\epsilon_0}{\epsilon_T(\mathbf{q},\omega)}\sum_\nu|M_\nu(\mathbf{q})|^2\ , \tag{3.20}$$

$$D_0(\mathbf{q},\omega)=\frac{1}{\omega-\omega_{\mathrm{ph}}+j0^+}-\frac{1}{\omega+\omega_{\mathrm{ph}}+j0^+}\ , \tag{3.21}$$

with $\bar{U}_0(\mathbf{q})=4\pi e^2/q^2$. Here $\bar{U}_0(\mathbf{q})/V$ and $\bar{U}_T(\mathbf{q})/V$ are the Fourier components of the bare interaction $e^2/|\mathbf{r}_1-\mathbf{r}_2|$ and of the screened interaction, respectively, between electrons at $\mathbf{r}_1$ and $\mathbf{r}_2$, $M_\nu(\mathbf{q})$ the matrix element for the electron-phonon interaction in the phonon mode

ν, $D_0(\mathbf{q},\omega)$ the free-particle Green's function for the phonon, and $\epsilon_T(\mathbf{q},\omega)$ the sum of the free-carrier screening and antiscreening due to the Coulomb interaction and the electron-phonon interaction, respectively. In $D_0(\mathbf{q},\omega)$, $\omega_{\rm ph}$ is the phonon energy which is assumed to be constant and equal for all phonon modes. As for $\epsilon_T(\mathbf{q},\omega)$, we have

$$\epsilon_T(\mathbf{q},\omega)=\epsilon(\mathbf{q},\omega)-\epsilon_0 D_0(\mathbf{q},\omega)\chi(\mathbf{q})\sum_\nu |M_\nu(\mathbf{q})|^2 \tag{3.22}$$

correcting an error in Ref. 30 as for this equation, where $\epsilon(\mathbf{q},\omega)$ is the sum of the free-carrier screening and the screening due to the host lattice; $V\chi(\mathbf{q})$ comes from the polarization diagram for the free-carrier screening. With the use of the Thomas-Fermi approximation and with the neglect of the retardation effect in the screening, we have $\lambda^2=-4\pi e^2\chi(0)/\epsilon_0$ and $\epsilon(\mathbf{q},\omega)=\epsilon_0(1+\lambda^2/q^2)$, so that we obtain

$$\epsilon_T(\mathbf{q},0)=\epsilon_0\left[1+\frac{\lambda^2}{q^2}-\frac{\epsilon_0\lambda^2}{2\pi e^2\omega_{\rm ph}}\sum_\nu |M_\nu(\mathbf{q})|^2\right] . \tag{3.23}$$

Considering the acoustic phonon scattering ($M_{\rm ac}$), the nonpolar optical phonon scattering ($M_{\rm npo}$), and the polar optical phonon scattering ($M_{\rm po}$), we give[32] $|M_{\rm ac}|^2=\Xi^2\omega_{\rm ph}/(2c_l)$, $|M_{\rm npo}|^2=E_{\rm npo}^2\omega_{\rm ph}/(2\bar{c})$, and $|M_{\rm op}|^2=2\pi e^2\omega_{\rm ph}/(\epsilon^* q^2)$, where $\Xi_{\rm ac}$ is the acoustic deformation potential, $E_{\rm npo}$ the nonpolar optical deformation potential, c_l the longitudinal spherical average elastic constant, $\bar{c}$ the averaged elastic constant, and $(\epsilon^*)^{-1}=\epsilon_\infty^{-1}-\epsilon_0^{-1}$ with ϵ_∞ as the high-frequency dielectric constant due to the host lattice. Then Eq. (3.23) is rewritten as

$$\epsilon_T(\mathbf{q},0)=\epsilon_{\rm eff}\left[1+\frac{\lambda_{\rm eff}^2}{q^2}\right] , \tag{3.24}$$

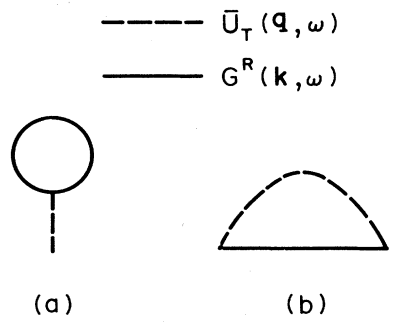

FIG. 1. Diagrams representing the terms of the electron-electron interaction in the lowest order in $\bar{U}_T(\mathbf{q},\omega)$.

$$\epsilon_{\rm eff}=\epsilon_0\left[1-\frac{\epsilon_0\lambda^2}{4\pi e^2}\left[\frac{\Xi^2}{c_l}+\frac{E_{\rm npo}^2}{\bar{c}}\right]\right] , \tag{3.25}$$

$$\lambda_{\rm eff}^2=\lambda^2\left[1-\frac{\epsilon_0}{\epsilon^*}\right] . \tag{3.26}$$

Equation (3.24) gives the modified form of the Thomas-Fermi screening, where the electron-electron attraction via the electron-phonon interaction leads to the antiscreening in contrast to the case of the Coulomb repulsion. We use $\epsilon_{\rm eff}$ and $\lambda_{\rm eff}$ in place of ϵ_0 and λ, respectively, in the calculations.

Now $\Sigma_r^R(\mathbf{k},\omega)$ in Eq. (3.8) is given with the use of Eq. (3.18) considering the diagrams shown in Fig. 1. As for Fig. 1(a), we omit the term of the electron-electron repulsion, i.e., the first term in Eq. (3.18), because this term has already been included in Eq. (3.4) in terms of Eq. (3.2). As for Fig. 1(b), we include the Coulomb-hole term coming from the plasmon pole.[33] As a result we obtain Σ_r^R as a sum of Σ_n ($n=1,2,3,4$), where

$$\Sigma_1=n_i[\bar{U}_T(0,0)-\bar{U}(0,0)] , \tag{3.27}$$

$$\Sigma_2=\frac{1}{\pi V}\sum_{\mathbf{q}}\int_{-\infty}^{\omega_F} d\omega\, \bar{U}_T(\mathbf{q},0)\,{\rm Im}G^R(\mathbf{k}-\mathbf{q},\omega) , \tag{3.28}$$

$$\Sigma_3=-\frac{\omega_p^2}{2V}\sum_{\mathbf{q}}\frac{4\pi e^2}{\epsilon_0 q^2\omega_1}{\rm Re}G^R(\mathbf{k}-\mathbf{q},\omega-\omega_1) , \tag{3.29}$$

$$\Sigma_4=\frac{\omega_p^2}{V}\sum_{\mathbf{q}}\frac{1}{\omega_1}\sum_\nu |M_\nu(q)|^2\left[\frac{\omega_{\rm ph}}{\omega_1^2-\omega_{\rm ph}^2}{\rm Re}G^R(\mathbf{k}-\mathbf{q},\omega-\omega_1)+\frac{\omega_1}{\omega_{\rm ph}^2-\omega_1^2}{\rm Re}G^R(\mathbf{k}-\mathbf{q},\omega-\omega_{\rm ph})\right] . \tag{3.30}$$

Here ω_p is the plasma frequency given by $\omega_p^2=4\pi e^2 n_i\hbar/(\epsilon_0 m_C)$ and $\omega_1^2=\omega_p^2(1+q^2/\lambda^2)+[E(\mathbf{q})]^2$. Equations (3.28)–(3.30) have been given for the original coordinate system of $\mathbf{q}$ and $\mathbf{k}$, as used in Eq. (2.19). In practical calculations, $\mathbf{q}$ and $\mathbf{k}$ are rewritten in the new coordinate system, as defined just below Eq. (2.19). In obtaining Eqs. (3.28)–(3.30) we have neglected the imaginary part of Σ_n's, whose effects are negligibly small as compared with that of the impurity scattering. Equation (3.27) and Eqs. (3.28)–(3.30) come from Figs. 1(a) and 1(b), respectively. Equations (3.29) and (3.30) come from the first term and the second term, respectively, of Eq. (3.18), taking into account the poles of ϵ_T^{-1} and of D_0. Actually we use G_0^R in place of G^R in all the equations for simplicity.

The dependence of the conductivity on the impurity species having the same valency in a given material is considered, as has been discussed[29]. We consider isocoric and nonisocoric impurities[34] which have the same cores and the different cores as that for the host lattice, respec-

tively. In order to take into account the core effect, we consider m_D to depend on the energy as in the method of Ref. 29. We give energy-dependent $m_D(\omega)$ as

$$m_D(\omega)=m_D, \quad \omega \geq \omega_c$$
$$m_D(\omega)=m_D'+(m_D-m_D')\exp\left[\frac{\omega-\omega_c}{2E_b}\right] \quad \omega<\omega_c \tag{3.31}$$

where E_b is the binding energy of an isolated impurity,

$$\omega_c=\frac{e^2\lambda}{\epsilon_0}\gamma+\Sigma_{xc} \tag{3.32}$$

with Σ_{xc} being defined as the shift of the band at an energy $(e^2\lambda/\epsilon_0)\gamma$ due to $\Sigma_r^R(\mathbf{k},\omega)$, and

$$m_D'=\frac{E_b(\text{nonisocore})}{E_b(\text{isocore})}m_D \tag{3.33}$$

for a multivalley semiconductor. The values of E_b's are obtained from experimental data on isocoric and nonisocoric impurities. For the valence band, we calculate m_D' directly from $m_D'=\hbar^2\epsilon_0/(a_D'e^2)$ with a_D' calculated from $E_b=e^2/(2\epsilon_0 a_D')$ with the use of E_b obtained from experimental data. With the use of $m_D(\omega)$ in place of m_D in various expressions such as Eqs. (3.12) and (3.13), the DOS and the conductivity are calculated.

IV. RESULTS AND DISCUSSION

In this section the theory in the previous sections is applied to various materials at 0 K. Especially, important parameters used for the calculations such as m_C, m_D, m_D', and E_b are shown in Table I. For materials where experimental data of E_b are not found, $m_D'=m_D$ is assumed and E_b is calculated from $E_b=e^2/(2\epsilon_0 a_D')$. Experimental data on some of the parameters and other parameters concerning the electron-phonon interaction are found in Refs. 8, 9, 35, and 36.

The resistivity is calculated as a function of the doping level up to the critical value n_c for the metal-insulator transition. Here, n_c is obtained from experimental data or from the relation[37]

$$a_D' n_c^{1/3}=0.25$$

with $a_D'=\hbar^2\epsilon_0/(m_D'e^2)$ unless experimental data are available.

First of all we discuss the calculation of the DOS and the conductivity for which the usual degeneracy of $f(\omega)=2\nu$ is assumed. In order to compare the present calculation with the previous ones we use $m_\perp=m_\parallel=m_C=m_D=0.48$ especially for p-type GaAs, take $\Sigma_r^R=0$, and neglect the effect of the electron-phonon interaction. Figure 2 shows the DOS for p-type GaAs under $n_i=5.4\times10^{18}$ cm^{-3} with $\omega=0$ at the unperturbed band edge. The solid line and the dashed line show the results of the present theory and of the BB theory, respectively. The solid circles[38] show experimental data, which have been obtained for Zn-doped GaAs from tunneling experiments at 4.2 K. The data are plotted so that an experimental value at an energy lying sufficiently deep in the band may fit the value in the present theory. It is seen that the DOS in the present theory is a few times larger than that in the BB theory especially in the range of $\omega<0$. Thus the present theory explains the experimental results better than the BB theory. However, the peak found in the experimental data is not obtained in both theories. The reason may be that we have used the average Green's function.

Figure 3 shows comparison of the present theory (solid

TABLE I. Material parameters.

Material	Dopant	m_c[a]	m_D[a]	m_D'[a]	ϵ_0	ν	E_b (meV)
Ge	P	0.12	0.22	0.21	15.4	4	12.0
Ge	As	0.12	0.22	0.22	15.4	4	12.7
Ge	Sb	0.12	0.22	0.17	15.4	4	9.7
Si	P	0.26	0.33	0.33	11.4	6	45.3
Si	As	0.26	0.33	0.39	11.4	6	53.5
Si	Sb	0.26	0.33	0.31	11.4	6	43
Si	Bi	0.26	0.33	0.50	11.4	6	69
GaAs	n type	0.067	0.067	0.067	12.8	1	
InP	n type	0.082	0.082	0.082	12.4	1	
GaSb	n type	0.042	0.042	0.042	15.7	1	
Ge	Al	0.31	0.36	0.18	15.4	1	10.2
Ge	B	0.31	0.36	0.18	15.4	1	10.4
Ge	In	0.31	0.36	0.20	15.4	1	11.2
Ge	Ga	0.31	0.36	0.19	15.4	1	11.0
Si	Al	0.49	0.53	0.54	11.4	1	57
Si	B	0.49	0.53	0.44	11.4	1	46
Si	Ga	0.49	0.53	0.68	11.4	1	71
GaAs	Zn	0.48	0.48	0.37	12.8	1	30.8
GaP	Zn	0.54	0.54	0.56	10.8	1	62
InP	Zn	0.65	0.65	0.35	12.4	1	31
InSb	Zn	0.40	0.40	0.21	17.9	1	9.0

[a]The mass is in unit of the electron mass *in vacuo*.

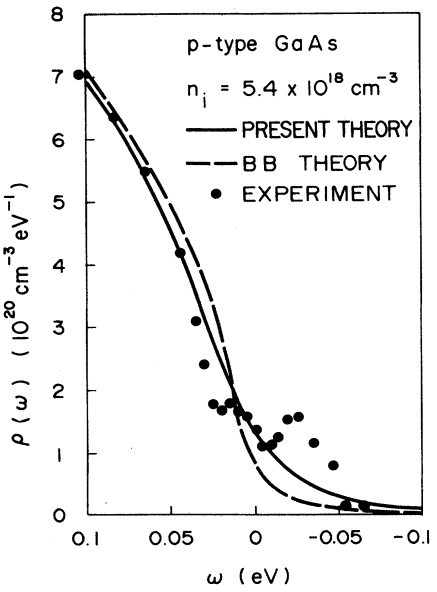

FIG. 2. DOS's vs the energy which are obtained for p-type GaAs with the acceptor concentration of 5.4×10^{18} cm^{-3} by the present theory (solid line), by the BB theory (dashed line), and from experiments (solid circles).

line) with earlier calculations[22,23] based on various other theories for the DOS in p-type GaAs at 0 K with $n_i=1.6\times10^{19}$ cm^{-3}. The latter theories are the BB theory (dotted line), Kane's theory (dotted-dashed line), and the Halperin–Lax–Sa-yakanit–Glyde theory[20,21] (dashed line). All these theories are found to give much smaller values of the DOS than the present theory in the range $\omega<0$.

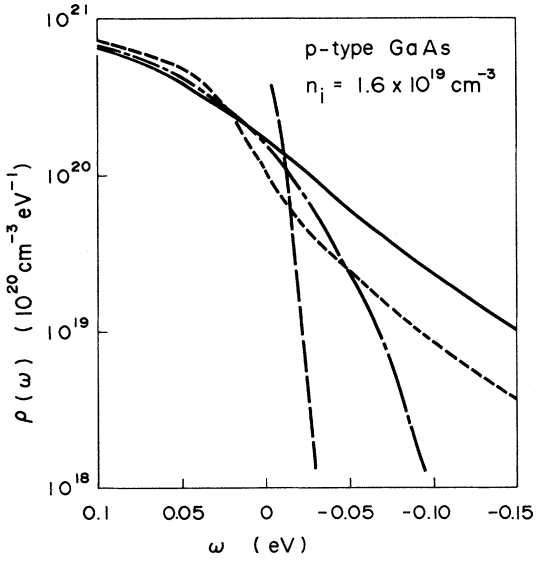

FIG. 3. DOS's vs the energy which are obtained for p-type GaAs with the acceptor concentration of 1.6×10^{19} cm^{-3} by the present theory (solid line), by the BB theory (dotted line), by the Kane's theory (dotted-dashed line), and by the Halperin–Lax–Sa-yakanit–Glyde theory (dashed line).

Now the present theory is applied to the calculation of the conductivity in n-type Ge and n-type Si at 0 K, for which experimental data at 4.2 K are available. We use material parameters in Table I and take $\Sigma_r^R=0$. We consider only isocoric impurities, i.e., As in Ge and P in Si. Figure 4 shows the resistivity plotted versus the doping level exceeding the critical value for the metal-insulator transition on Ge:As. The solid line and the dashed line show the results of the present theory and the BB theory, respectively. Experimental data are shown by the open rectangles[10] and the open triangles.[39] As is seen, although the BB theory explains considerably well the experimental data,[40] the present theory gives a worse explanation of the data.

The above situation is seen also in other materials such as n-type Si. Figure 5 shows the resistivity plotted versus the doping level exceeding the critical value for the metal-insulator transition on Si:P. The solid line and the dashed line show the results of the present theory and the BB theory, respectively. The solid circles show experimental data.[41] As is seen, the present theory gives a worse explanation of the experimental data than the BB theory.

As has been seen above, the present theory gives larger DOS's in the band-tail region and larger resistivities than the BB theory. This is a consistent result in the respect that an increased effect of the impurity scattering in the present theory leads to increased DOS's and increased resistivities as compared with the case of the BB theory. The increased DOS has been found to better explain the experimental data. However, a difficulty is that the BB theory better explains the experimental data of the con-

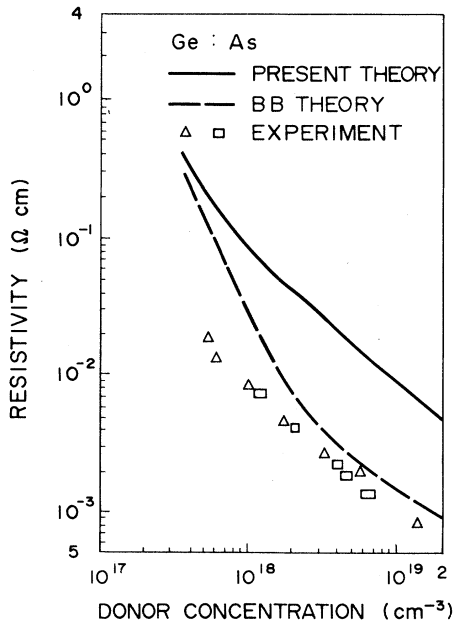

FIG. 4. Resistivities vs the donor concentration which are obtained for Ge:As by the present theory (solid line), by the BB theory (dashed line), and from experiments (open triangles and open rectangles).

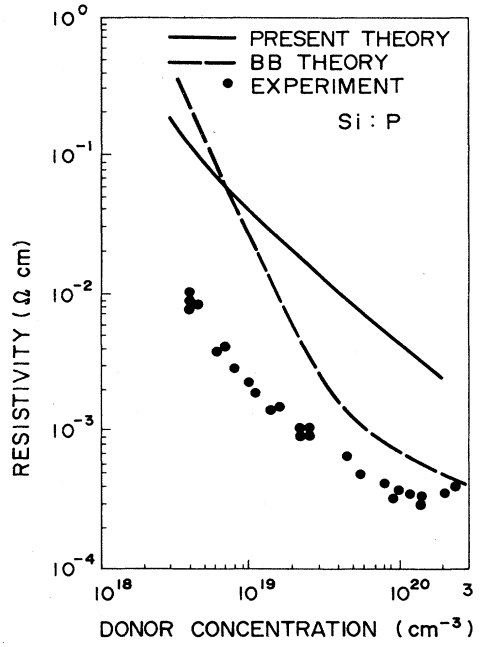

FIG. 5. Resistivities vs the donor concentration which are obtained for Si:P by the present theory (solid line), by the BB theory (dashed line), and from experiments (solid circles).

ductivity than the present theory. This is curious from the viewpoint that the present theory is more rigorous than the BB theory. On the other hand, it is found that the SP theory[22,23] gives nearly the same DOS as the present theory. It is found also that the SP theory gives a worse explanation of experimental results on some electronic properties such as the conductivity, the Auger recombination[26], and the intervalence band absorption[42] than the BB theory. The SP theory is another approach giving the quantum correction to the BB model. Therefore, the difficulty stated above is common to both the quantum and the SP approaches giving the quantum correction.

The decrease of the conductivity in the quantum theory relative to that in the BB theory occurs through the decrease of the Fermi level resulting from the increase of the DOS in the band-tail region and through the decrease of the peak height of $-\mathrm{Im}\bar{G}^{R}(\Omega,k)$ resulting from the increase of the width of the function; an inverse relation between the peak height and the width is understood from the relation

$$-\int_{-\infty}^{\infty} d\Omega\, \mathrm{Im}\bar{G}^{R}(\Omega,k)=\pi \tag{4.1}$$

for a given k. In order to give a satisfactory explanation of experiments still within the framework of the quantum theory, therefore, there should be some situation where the DOS, especially in the band-tail region, is smaller, still remaining close to the experimental one. This situation, which might seem contradictory, is found by considering both localized states at low energies and Σ_r^R given as a sum of Eqs. (3.27)–(3.30). Thus the theory is improved as is seen below.

Although the quantum theory never leads directly to localized states, it is considered that the localization occurs at energies below some critical value. The reason why the theory does not lead to the localization may be the use of the vertex part of the two-particle Green's function simply in the BB theory and of the ensemble-averaged Green's function. In view of this it is assumed that we have localized states at energies below some critical value and that the degeneracy for each localized state is unity in place of 2ν. The latter assumption is based on the same situation[43] found on localized donors and acceptors. The critical energy for the localization lies in between the band edge and the ground level of an isolated impurity. The band shift due to the Coulomb term of the electron-electron interaction is found to be $(e^2\lambda/\epsilon_0)\gamma$ by hypothetically setting $U_i(r)$ to be zero in Eq. (2.22) and by neglecting Σ_r^R. In considering Σ_r^R, therefore, the shifted band edge is at ω_c given by Eq. (3.32) as measured from the unperturbed band edge. The critical energy for the localization is assumed to lie in between ω_c and ω_c-E_b. For $\omega>\omega_c$ we have $f(\omega)=2\nu$ while for $\omega<\omega_c-E_b$ we have $f(\omega)=1$. An abrupt jump from 2ν to 1 may occur at a critical energy in between ω_c and ω_c-E_b. However, only because we have no precise information of the critical energy, we assume a somewhat gradual variation of $f(\omega)$ according to

$$\begin{aligned} &f(\omega)=2\nu, \quad \omega\geq\omega_c \\ &f(\omega)=1+(2\nu-1)\exp\left[\frac{\omega-\omega_c}{2E_b}\right], \quad \omega<\omega_c\ . \end{aligned} \tag{4.2}$$

We use this new definition of $f(\omega)$ and consider Σ_r^R for the improved calculation below. The effect of Σ_r^R is to cause the shift of the DOS towards a lower energy region as compared with the case of neglected Σ_r^R. This shift tends to compensate for the decrease of the DOS under $f(\omega)$ above. The effect of the electron-phonon interaction is considered. Let us call hereafter the improved theory above and the theory before the improvement as the present theory and the previous theory, respectively.

First we compare the present theory with experiments on the resistivity in materials for which experimental data at low temperatures are available. Figures 6–8 show the resistivities as functions of the doping level which are obtained from the present theory (lines) with experiments (points). In Fig. 6, the solid line, the open triangles,[39] and the open rectangles[10] are for Ge:As, the dashed line, the solid triangles,[39] the solid rectangles,[10] and the solid circles[44] are for Ge:Sb, and the dotted line is for Ge:P. In Fig. 7, the solid line and the solid circles[41] are for Si:P, the dashed line and the open circles[45] are for Si:As, the dotted-dashed line is for Si:Sb, and the dotted line is for Si:Bi. In Fig. 8, the solid line is for Ge:Ga, Ge:In, Ge:Al, and Ge:B, and the solid circles[44] are for Ge:Ga. It is seen that agreement between the theory and experiments is considerably good for all the materials shown.

Figure 9 shows comparison of the result in the present theory using Σ_r^R (solid line) with those in the same theory especially under the neglect of Σ_r^R (the dotted-dashed line), in the previous theory (dashed line), and in the BB

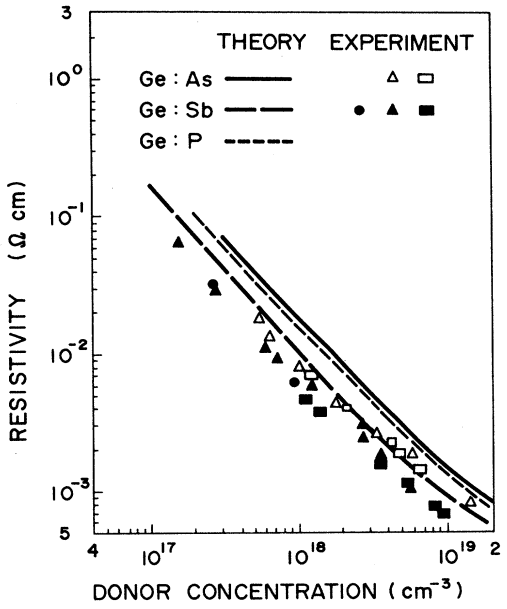

FIG. 6. Resistivities vs the donor concentration which are obtained by the present theory (lines) and from experiments (points) for Ge:As (solid line, open triangles, open rectangles), for Ge:Sb (dashed line, solid circles, solid triangles, solid rectangles), and for Ge:P (dotted line).

theory[28] (dotted line) on the resistivity in Ge:As; the open triangles and the open rectangles show the same experimental data as shown in Fig. 6. It is seen that the present theory gives the best explanation of the experimental data and that the contribution of Σ_r^R to the conductivity is significant but small as compared with that of $f(\omega) \neq 2\nu$.

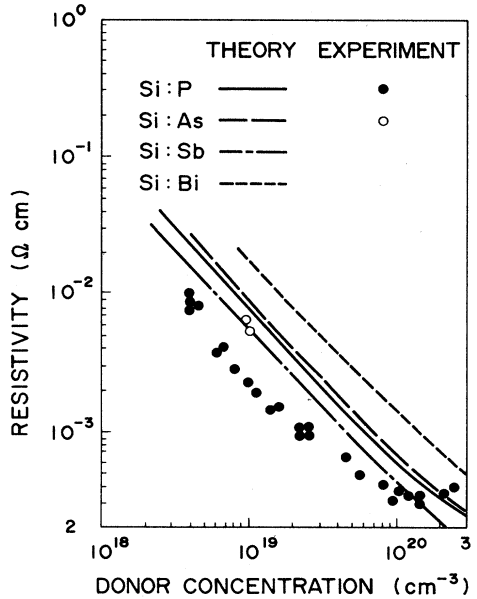

FIG. 7. Resistivities vs the donor concentration which are obtained by the present theory (lines) and from experiments (points) for Si:P (solid line, solid circles), for Si:As (dashed line, open circles), for Si:Sb (dotted-dashed line), and for Si:Bi (dotted line).

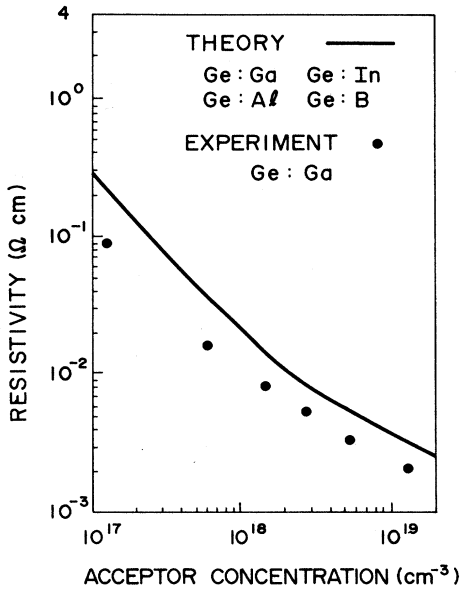

FIG. 8. Resistivities vs the acceptor concentration which are obtained by the present theory (solid line) for Ge:Ga, Ge:In, Ge, Al, and Ge:B, and from experiments on Ge:Ga (solid circles).

This situation is the same for other materials. Thus the present theory is most useful for explaining the experimental data of the resistivity. Stimulated by the success, the resistivities in the present theory are shown also in Figs. 10–12 for p-type Si, n-type III-V compounds, and p-type III-V compounds, respectively.

Figure 13 shows the DOS's in p-type GaAs doped with

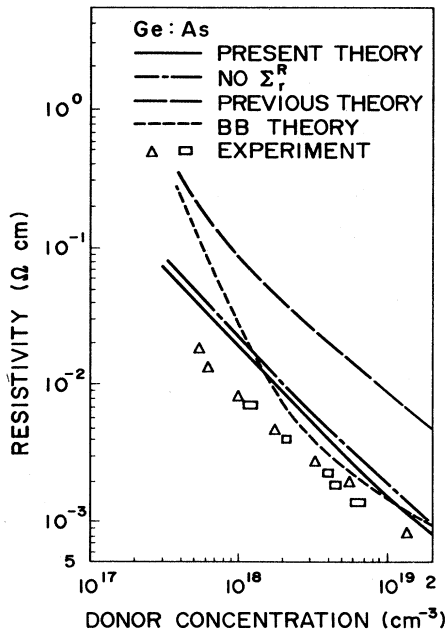

FIG. 9. Resistivities vs the donor concentration which are obtained for Ge:As by the present theory with (solid line) and without (dotted-dashed line) Σ_r^R, by the previous theory (dashed line), by the BB theory (dotted line), and from experiments (open triangles, open rectangles).

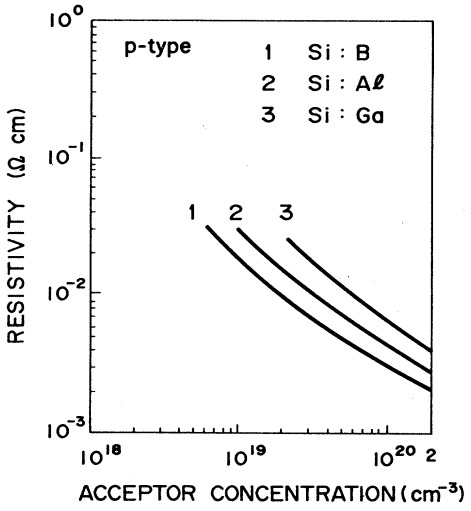

FIG. 10. Resistivities vs the acceptor concentration which are obtained for p-type Si doped with B, Al, and Ga by the present theory.

Zn under $n_i = 5.4 \times 10^{18}$ cm^{-3} as functions of the energy ω. The solid line, the dashed line, and the dotted line show results in the present theory, in the previous theory, and in the BB theory, respectively. The solid circles show the same experimental data as shown in Fig. 2. It is seen that the present theory gives the results closest to the experimental data.

Figure 14 shows the DOS's calculated from the present theory for p-type GaAs with $n_i = 5.4 \times 10^{18}$ cm^{-3} under various assumptions. The dashed line, the dotted line, and the solid line show the results obtained by neglecting the phonon effects, by neglecting Σ_r^R, and by including all these effects, respectively. Correspondingly to the cases of the solid line, the dashed line, and the dotted line, we find the resistivities 0.024, 0.027, and 0.036 Ω cm, respectively, together with $\omega_F = 11.8$, 27.2, and 36.2 meV, respectively. In view of this result and of results in Fig. 13, the phonon effect as well as that of Σ_r^R is not negligible. Especially, the result in Fig. 13 that the DOS at $\omega < 0$ is larger in the present theory than in the previous theory is ascribed to the inclusion of Σ_r^R, which causes the band to shift towards a lower energy region.

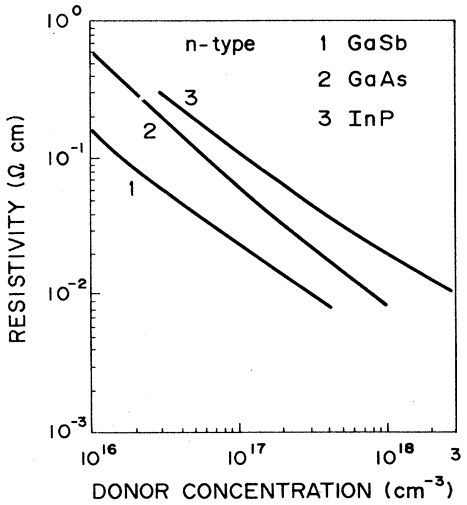

FIG. 11. Resistivities vs the donor concentration which are obtained for n-type III-V compounds of GaSb, GaAs, and InP by the present theory.

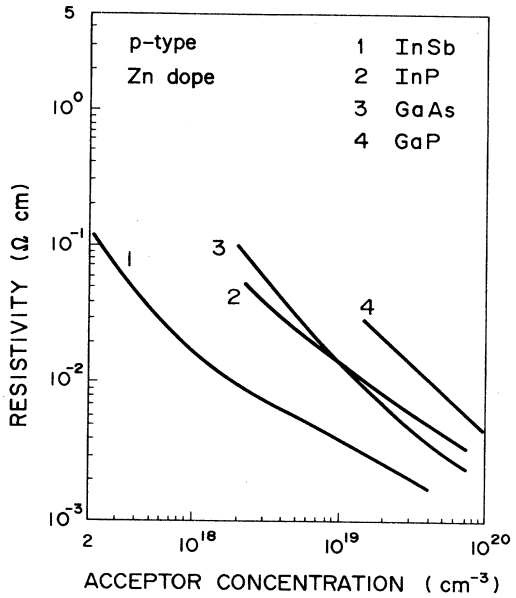

FIG. 12. Resistivities vs the acceptor concentration which are obtained for Zn-doped p-type III-V compounds of InSb, InP, GaAs, and GaP by the present theory.

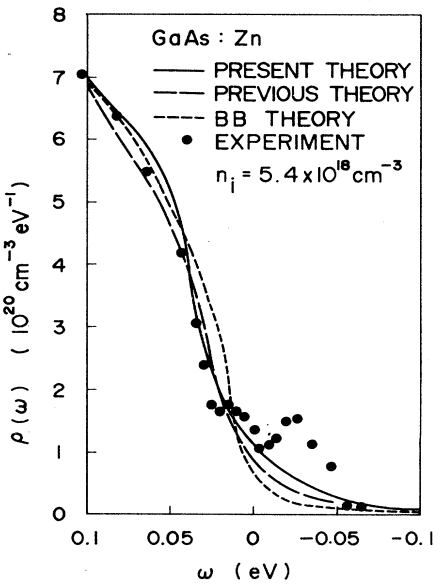

FIG. 13. DOS's vs the energy which are obtained for p-type GaAs doped with Zn at the level of 5.4×10^{18} cm^{-3} by the present theory (solid line), by the previous theory (dashed line), by the BB theory (dotted line), and from experiments (solid circles).

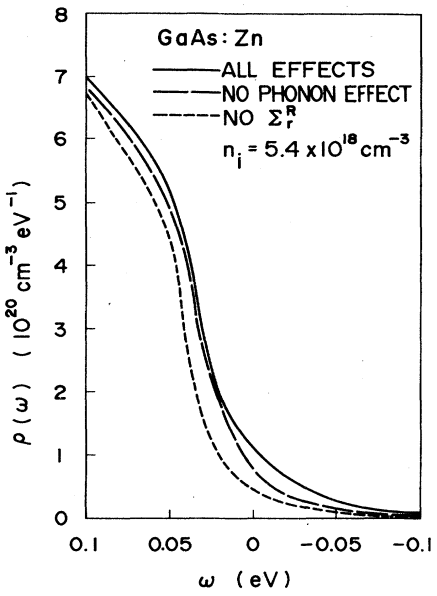

FIG. 14. DOS's vs the energy which are obtained for p-type GaAs doped with Zn at the level of 5.4×10^{18} cm^{-3} by the present theory, neglecting the phonon effect (dashed line) or Σ_r^R (dotted line), and taking into account all the effects (solid line).

Although the present theory has been found to give a considerably good explanation of experiments, there are still many shortcomings in the theory. First, Eq. (3.10) for λ has been given by neglecting[28] the vertex part of the two-particle Green's function. This neglected part might be important around the metal-insulator transition, possibly reducing λ. However, the Thomas-Fermi approximation, where the screening is described simply by λ, is supported by the results of the calculation made also under the Lindhart potential. It is found that the resistivities calculated under the Lindhart potential with the use of λ given by Eq. (3.10) are practically the same as those under the Thomas-Fermi potential. Second, the vertex part of the conductivity σ_2 has been calculated simply in the BB model, and not in the quantum model. Because σ_2 is an important parameter describing the localization, the quantum theoretical calculation of σ_2 may be important especially around the metal-insulator transition or at energies below some value. Third, the Green's function has been calculated under an ensemble average over the impurity sites assuming uniform probability of the distribution. This procedure gives the smoothing of the random impurity distribution so that the effect of isolated impurities or small clusters of them cannot be included correctly. In fact, the calculated DOS shows simply a monotonic decrease with decreasing ω in the range $\omega<0$ where the experimental DOS shows a peak in contrast, as shown in Fig. 13.

The above shortcomings altogether may lead to the failure of the theory in describing the localization. In fact, the theory never shows a rapid decrease of the conductivity to zero with decreasing impurity concentration even around the metal-insulator transition observed experimentally. The semiempirical form of $f(\omega)$ is provided as a simple cure for the shortcoming. Naturally, there is a considerable uncertainty in the semiempirical determination of $f(\omega)$, as the fourth shortcoming of the theory. Further, we have not taken into account the requirement that the decrease of $f(\omega)$ to values less than 2ν in the range $\omega<\omega_c$ should be compensated by the increase of $f(\omega)$ to values larger than 2ν in the range $\omega<\omega_c$. As a result the Fermi level is overestimated, which may influence the calculated conductivity. Despite the above shortcomings, the calculations based on the assumed form of $f(\omega)$ have been found to lead to considerably satisfactory results. It is concluded therefore that the quantum theory of electronic properties based on the one-particle Green's function is useful under the assumption of localized states with the use of the semiempirical form of the energy-dependent degeneracy although the development of a more rigorous theory still remains as a future program.

ACKNOWLEDGMENTS

The author wishes to express his appreciation to Dr. G. Kano and Dr. I. Teramoto for their constant encouragement.

APPENDIX A: CALCULATION OF THE $K_n(\mathbf{k})$ ENTERING $G^R(\mathbf{k})$

We derive an expression for the one-particle Green's function $G^R(\mathbf{k})$, calculating $K_1(\mathbf{k})$ and $K_2(\mathbf{k})$, and then extending the calculation to $K_n(\mathbf{k})$ for $n\geq3$ as follows.

First we calculate $K_1(\mathbf{k})$ in Eq. (2.14). Using a new definition $O_p(\mathbf{k}+j\nabla)=E(\mathbf{k}+j\nabla)-E(\mathbf{k})$ for convenience, let us start with

$$K_1(\mathbf{k},\mathbf{k}')=[G_0^R(\mathbf{k})]^2\frac{1}{V}\sum_{m=0}^{\infty}\sum_{n=0}^{\infty}d\mathbf{r}\exp[-j(\mathbf{k}-\mathbf{k}')\cdot\mathbf{r}][G_0^R(\mathbf{k})\Gamma(\mathbf{r})]^m O_p(\mathbf{k}+j\nabla)[G_0^R(\mathbf{k})\Gamma(\mathbf{r})]^n\,, \tag{A1}$$

which is obtained from Eq. (2.13). With the use of Eq. (2.2), the above equation is rewritten as

$$K_1(\mathbf{k},\mathbf{k}')=[G_0^R(\mathbf{k})]^2\sum_{m=0}^{\infty}\sum_{n=0}^{\infty}\sum_{\mathbf{q}_1\mathbf{q}_2\cdots\mathbf{q}_m}\sum_{\mathbf{p}_1\mathbf{p}_2\cdots\mathbf{p}_n}\Delta(\mathbf{Q}_m+\mathbf{P}_n+\mathbf{k}-\mathbf{k}')O_p(\mathbf{k}-\mathbf{P}_n)\prod_{\mu=1}^{m}[G_0^R(\mathbf{k})\bar{\Gamma}(\mathbf{q}_\mu)]\prod_{\nu=1}^{n}[G_0^R(\mathbf{k})\bar{\Gamma}(\mathbf{p}_\nu)]\,, \tag{A2}$$

where $\mathbf{Q}_m$, $\mathbf{P}_n$, $\mathbf{q}_\mu$, and $\mathbf{p}_\nu$ are the wave vectors with $\mathbf{Q}=\sum_{\mu=1}^{m}\mathbf{q}_\mu$ and $\mathbf{P}_n=\sum_{\nu=1}^{n}\mathbf{p}_\nu$. The terms of $K_1(\mathbf{k})$ which are obtained from this relation by taking on ensemble average of $K_1(\mathbf{k},\mathbf{k}')$ are diagrammatically shown in Fig. 15, where the

solid lines show $G_0^R(\mathbf{k})$, the crosses the impurity sites with each site assigned with N_i, and the dotted lines the electron-impurity interaction $\bar{U}_i(\mathbf{q})/V$ defined as

$$U_i(\mathbf{r})=\frac{1}{V}\sum_{\mathbf{q}}\bar{U}_i(\mathbf{q})\exp(j\mathbf{q}\cdot\mathbf{r})\ . \tag{A3}$$

The upper line and the lower line in Fig. 15 come from the factors $\prod_{\mu=1}^{m}[G_0^R(\mathbf{k})\bar{\Gamma}(\mathbf{q}_\mu)]$ and $\prod_{\nu=1}^{n}[G_0^R(\mathbf{k})\bar{\Gamma}(\mathbf{p}_\nu)]$, respectively, in Eq. (A2). As shown in the figure, the impurity sites are classified into three groups. In one group denoted $b=1$, each impurity site is connected to both the upper solid line and the lower solid line via the interaction lines. In the other groups, $b=2$ or $b=3$, each impurity site is connected either to the upper solid line or to the lower solid line, respectively. We write the number of the impurity sites in a group b as a_b $(b=1,2,3)$.

The calculation is quite similar to that for the two-particle Green's function in the BB approach. Let us define

$$H(\mathbf{Q}_m,\mathbf{P}_n)=\Delta(\mathbf{Q}_m+\mathbf{P}_n)\prod_{\mu=1}^{m}\left[\frac{\bar{U}_i(\mathbf{q}_\mu)}{V}\right]\prod_{\nu=1}^{n}\left[\frac{\bar{U}_i(\mathbf{p}_\nu)}{V}\right]\ ; \tag{A4}$$

especially for $n=0$ as an example we define $H(\mathbf{Q}_m,0)=\Delta(\mathbf{Q}_m)\prod_{\mu=1}^{m}[\bar{U}_i(\mathbf{q}_\mu)/V]$. Then the diagram in Fig. 15 gives a term for $K_1(\mathbf{k})$ as

$$S(\mathbf{M},\mathbf{N})=[G_0^R(\mathbf{k})]^{M+N+2}\sum_{(\mathbf{q})(\mathbf{p})}\Delta(\mathbf{Q}+\mathbf{P})O_p(\mathbf{k}-\mathbf{P})\prod_{b=1}^{3}\left[(N_i)^{a_b}\prod_{c=1}^{a_b}H(\mathbf{Q}_{bm_{bc}},\mathbf{P}_{bm_{bc}})\right], \tag{A5}$$

where $\mathbf{Q}_{bm_{bc}}$ ($\mathbf{P}_{bm_{bc}}$) is the sum of $\mathbf{q}$'s ($\mathbf{p}$'s) with the number of $\mathbf{q}$'s ($\mathbf{p}$'s) being m_{bc} (n_{bc}) for the interaction lines connected to the impurity site c in the group b, $\mathbf{Q}$ ($\mathbf{P}$) is the sum of all $\mathbf{q}$'s ($\mathbf{p}$'s), $\sum_{(\mathbf{q})(\mathbf{p})}$ means the summation over all $\mathbf{q}$'s and $\mathbf{p}$'s, $\mathbf{M}$ ($\mathbf{N}$) represents all m_{bc}'s (n_{bc}'s), and M (N) is the sum of all m_{bc}'s (n_{bc}'s). Especially we have $m_{3c}=0$ and $n_{2c}=0$ together with $\mathbf{P}_{20}=0$ and $\mathbf{Q}_{30}=0$. With the use of Eq. (A4),

$$\Delta(\mathbf{q})=\frac{1}{V}\int d\mathbf{r}\exp(j\mathbf{q}\cdot\mathbf{r})\ , \tag{A6}$$

$$\int d\mathbf{r}[U_i(\mathbf{r})]^m=V\sum_{\mathbf{q}_1\mathbf{q}_2\cdots\mathbf{q}_m}\Delta(\mathbf{q}_1+\mathbf{q}_2+\cdots+\mathbf{q}_m)\prod_{\mu=1}^{m}\left[\frac{\bar{U}_i(\mathbf{q}_\mu)}{V}\right], \tag{A7}$$

and

$$\Delta(\mathbf{Q}+\mathbf{P})O_p(\mathbf{k}-\mathbf{P})=\frac{1}{V}\int d\mathbf{r}\exp(j\mathbf{Q}\cdot\mathbf{r})O_p(\mathbf{k}+j\nabla)\exp(j\mathbf{P}\cdot\mathbf{r})\ , \tag{A8}$$

we obtain after some manipulation

$$S(M,N)=[G_0^R(\mathbf{k})]^2\int d\boldsymbol{\rho}_1\delta(\boldsymbol{\rho}_1)\int d\boldsymbol{\rho}_2\delta(\boldsymbol{\rho}_2)O_p\left[\mathbf{k}+j\frac{\partial}{\partial\boldsymbol{\rho}_2}\right]\prod_{b=1}^{3}\left[(n_i)^{a_b}\int\mathcal{D}\mathbf{r}_{a_b}\prod_{c=1}^{a_b}(u_{bc})^{m_{bc}}(v_{bc})^{n_{bc}}\right] \tag{A9}$$

under the definition of $u_{bc}=G_0^R(\mathbf{k})U_i(\mathbf{r}_{bc}+\boldsymbol{\rho}_1)$ for $b=1$ and 2, $u_{3c}=1$, $v_{bc}=G_0^R(\mathbf{k})U_i(\mathbf{r}_{bc}+\boldsymbol{\rho}_2)$ for $b=1$ and 3, and $v_{2c}=1$; n_i is the impurity concentration N_i/V and we define $\mathcal{D}\mathbf{r}_{a_b}=\prod_{c=1}^{a_b}d\mathbf{r}_{bc}$. We take $u_{3c}=v_{2c}=1$ in view of the fact that we have no corresponding diagrams in Fig. 15.

Defining $\bar{K}_1(\mathbf{k})$ by

$$K_1(\mathbf{k})=[G_0^R(\mathbf{k})]^2\int d\boldsymbol{\rho}_1\delta(\boldsymbol{\rho}_1)\int d\boldsymbol{\rho}_2\delta(\boldsymbol{\rho}_2)O_p\left[\mathbf{k}+j\frac{\partial}{\partial\boldsymbol{\rho}_2}\right]\bar{K}_1(\mathbf{k})\ , \tag{A10}$$

we have

$$\bar{K}_1(\mathbf{k})=\prod_{b=1}^{3}\left[\sum_{a_b=0}^{\infty}\frac{(n_i)^{a_b}}{a_b!}\sum_{\mathbf{M}}{}'P(\mathbf{M},M)\sum_{\mathbf{N}}{}'P(\mathbf{N},N)\int\mathcal{D}\mathbf{r}_{a_b}\prod_{c=1}^{a_b}(u_{bc})^{m_{bc}}(v_{bc})^{n_{bc}}\right], \tag{A11}$$

where

$$P(\mathbf{M},M)=M!\Big/\left[\prod_{b=1}^{3}\prod_{c=1}^{a_b}m_{bc}!\right] \tag{A12}$$

and $\sum_{\mathbf{M}}'$ means the summation over all m_{bc}'s under the restriction $m_{bc}\geq 1$; these situations are the same for $P(\mathbf{N},N)$ and $\sum_{\mathbf{N}}'$. It is easy to see that

$$\sum_{\mathbf{M}}{}' P(\mathbf{M},M)\prod_{b=1}^{2}\prod_{c=1}^{a_b}(u_{bc})^{m_{bc}}=\sum_{M_1+M_2=M}\frac{M!}{M_1!M_2!}\sum_{\mathbf{M}_1}{}' P(\mathbf{M}_1,M_1)\sum_{\mathbf{M}_2}{}' P(\mathbf{M}_2,M_2)\prod_{b=1}^{2}\prod_{c=1}^{a_b}(u_{bc})^{m_{bc}}\ , \tag{A13}$$

where $\mathbf{M}_l=(m_{l1},m_{l2},\ldots,m_{la_l})$, $M_l=\sum_{c=1}^{a_l}m_{lc}$, and $\sum'_{\mathbf{M}_l}$ means the summation over m_{lc}'s for a given M_l under $m_{lc}\geq 1$. We make use of the relation[28] for M_l with $l=1$ and 2

$$\sum_{\mathbf{M}_l}{}' P(\mathbf{M}_l,M_l)\prod_{\mu=1}^{a}(u_\mu)^{m_\mu}=\sum_{\mu=0}^{a-1}(-1)^\mu\sum_{(n)}(u_{n_1}+u_{n_2}+\cdots+u_{n_{a-\mu}})^{M_l}\ , \tag{A14}$$

where $\mathbf{M}_l=(m_1,m_2,\ldots,m_a)$, $M_l=\sum_{\mu=1}^{a}m_\mu$, $a\equiv a_l$ ($l=1$ or 2), each u_{n_α} ($\alpha=1,2,\ldots,a-\mu$) takes some one out of u_β's ($\beta=1,2,\ldots,a$), and $\sum_{(n)}$ means the summation over all possible choices of u_{n_α}'s out of u_β's under the restriction that u_{n_α} with smaller α is equal to u_β with smaller β. It should be noted that the right-hand side of Eq. (A14) is zero if we hypothetically take M_l in the range $1\leq M_l\leq a-1$. Therefore, M_l ($l=1,2$) in Eq. (A13) is allowed, after the substitution of Eq. (A14) into Eq. (A13), to be in the range $M_l\geq 1$ although actually Eq. (A13) makes sense only in the range $M_l\geq a$. As a result, M and N in Eq. (A11) are in the range $M\geq 2$ and $N\geq 2$. After some manipulation we obtain

$$\begin{aligned}\bar{K}_1(\mathbf{k})=&\prod_{b=1}^{3}\left[\sum_{a_b=0}^{\infty}\frac{(n_i)^{a_b}}{a_b!}\int\mathcal{D}\mathbf{r}_{a_b}\right]\sum_{M=2}^{\infty}\sum_{N=2}^{\infty}\sum_{(m)(n)}\sum_{\mu_1=0}^{a_1-1}(-1)^{\mu_1}\sum_{\mu_2=0}^{a_2-1}(-1)^{\mu_2}\sum_{\nu_1=0}^{a_1-1}(-1)^{\nu_1}\sum_{\nu_3=0}^{a_3-1}(-1)^{\nu_3}\\&\times\left[\left[\sum_{\sigma=1}^{a_1-\mu_1}u_{1,m_\sigma}+\sum_{\sigma=1}^{a_2-\mu_2}u_{2m_\sigma}\right]^M-\left[\sum_{\sigma=1}^{a_1-\mu_1}u_{1m_\sigma}\right]^M-\left[\sum_{\sigma=1}^{a_2-\mu_2}u_{2m_\sigma}\right]^M\right]\\&\times\left[\left[\sum_{\sigma=1}^{a_1-\nu_1}v_{1n_\sigma}+\sum_{\sigma=1}^{a_3-\mu_3}v_{3n_\sigma}\right]^N-\left[\sum_{\sigma=1}^{a_1-\nu_1}v_{1n_\sigma}\right]^N-\left[\sum_{\sigma=1}^{a_3-\nu_3}v_{3n_\sigma}\right]^N\right]\ ,\end{aligned} \tag{A15}$$

where $\sum_{(m)(n)}$ means the summation over all possible ways of choosing u_{cm_σ} ($\sigma=1,2,\ldots,a_c-\mu_c$) and v_{cn_σ} ($\sigma=1,2,\ldots,a_c-\nu_c$). We have no summations over μ_3 and ν_3 corresponding to the fact that we have no diagrams giving u_{3c} and v_{2c} in Fig. 15.

In Eq. (A15) the summation over M and N in the range $M\geq 2$ and $N\geq 2$ can be extended to that in the range $M\geq 1$ and $N\geq 1$ because the terms for $M=1$ and/or $N=1$ are absolutely zero. With the use of the relation

$$\frac{1}{1-u}=\frac{1}{jG_0^R(\mathbf{k})}\int_0^\infty ds\exp\left[\frac{js}{G_0^R(\mathbf{k})}(1-u)\right]\ , \tag{A16}$$

where $u=G_0^R(\mathbf{k})U$ with U as a real quantity, we obtain after performing the summation over M and N

$$\begin{aligned}\bar{K}_1(\mathbf{k})=&\left[\frac{1}{jG_0^R(\mathbf{k})}\right]^2\prod_{b=1}^{3}\left[\sum_{a_b=0}^{\infty}\frac{(n_i)^{a_b}}{a_b!}\int\mathcal{D}\mathbf{r}_{a_b}\right]\sum_{(m)(n)}\\&\times\sum_{\mu_1=0}^{a_1-1}(-1)^{\mu_1}\sum_{\mu_2=0}^{a_2-1}(-1)^{\mu_2}\sum_{\nu_1=0}^{a_1-1}(-1)^{\nu_1}\sum_{\nu_3=0}^{a_3-1}(-1)^{\nu_3}\int_0^\infty ds_1\int_0^\infty ds_2\exp\left[\frac{j}{G_0^R(\mathbf{k})}(s_1+s_2)\right]\\&\times\{[(F_{11}-1)(F_{12}-1)-1][(F_{21}-1)(F_{23}-1)-1]-1\}\ ,\end{aligned} \tag{A17}$$

where

$$\begin{aligned}F_{1b}=&\exp\left[\frac{js_1}{G_0^R(\mathbf{k})}\sum_{\sigma=1}^{a_b-\mu_b}u_{bm_\sigma}\right]\quad(b=1,2)\ ,\\F_{2b}=&\exp\left[\frac{js_2}{G_0^R(\mathbf{k})}\sum_{\sigma=1}^{a_b-\nu_b}v_{bn_\sigma}\right]\quad(b=1,3)\ .\end{aligned} \tag{A18}$$

The suffix b in F_{1b} and F_{2b} indicates that the integration variables $\mathbf{r}_{bc}$ ($c=1,2,\ldots,a_b$) for the integral $\int\mathcal{D}\mathbf{r}_{a_b}=\prod_{c=1}^{a_b}\int d\mathbf{r}_{bc}$ are contained in F_{1b} and F_{2b}. Thus F_{11} and F_{21} are linked in the sense that both are subject to the common integration, while F_{12} and F_{23} are not linked to any others. Noting this situation, Eq. (A17) is found to be given in terms of the factors

$$H_1(s_b)=\sum_{a_b=0}^{\infty}\frac{(n_i)^{a_b}}{a_b!}\sum_{(m)}\sum_{\mu_b=0}^{a_b-1}(-1)^{\mu_b}\int\mathcal{D}\mathbf{r}_{a_b}[F_{\beta b}(a_b-\mu_b)-1] \tag{A19}$$

with $\beta=1$ and 2, and

$$H_2(s_1,s_2)=\sum_{a_1=0}^{\infty}\frac{(n_i)^{a_1}}{a_1!}\sum_{(m)(n)}\sum_{\mu_1=0}^{a_1-1}(-1)^{\mu_1}\sum_{\nu_1=0}^{a_1-1}(-1)^{\nu_1}\int\mathcal{D}\mathbf{r}_{a_1}[F_{11}(a_1-\mu_1)-1][F_{21}(a_1-\nu_1)-1]\,, \tag{A20}$$

where F_{1b} and F_{2b} are expressed as functions of $a_b-\mu_b$ and $a_b-\nu_b$, respectively, noting Eq. (A18). Actually $H_1(s_b)$ is independent of $\boldsymbol{\rho}_1$ and $H_2(s_1,s_2)$ depends on $\boldsymbol{\rho}_1$ and $\boldsymbol{\rho}_2$. We find

$$H_1(s)=\exp[n_i V h_1(s)] \tag{A21}$$

with

$$h_1(s)=\frac{1}{V}\int d\mathbf{r}\{\exp[-jsU_i(\mathbf{r})]-1\}\,. \tag{A22}$$

As for $H_2(s_1,s_2)$, after slight modification as

$$H_2(s_1,s_2)=\sum_{a_1=0}^{\infty}\frac{(n_i)^{a_1}}{a_1!}\sum_{(m)(n)}\sum_{\mu_1=1}^{a_1}(-1)^{\mu_1}\sum_{\nu_1=1}^{a_1}(-1)^{\nu_1}\int\mathcal{D}\mathbf{r}_{a_1}F_{11}(\mu_1)F_{21}(\nu_1)\,, \tag{A23}$$

we obtain

$$H_2(s_1,s_2)=\sum_{a_1=0}^{\infty}(n_i V)^{a_1}\sum_{m_1=0}^{a_1}\sum_{m_2=0}^{a_1-m_1}\sum_{m_3=0}^{a_1-m_1}\frac{1}{m_1!m_2!m_3!(a_1-m_1-m_2-m_3)!}$$
$$\times[h_2(s_1,s_2)+1]^{m_1}[-h_1(s_1)-1]^{m_2}[-h_1(s_2)-1]^{m_3} \tag{A24}$$

under $a_1-m_1-m_2-m_3\geq 0$, where

$$h_2(s_1,s_2)=\frac{1}{V}\int d\mathbf{r}\{\exp[-jU_i(\mathbf{r}+\boldsymbol{\rho}_1)s_1-jU_i(\mathbf{r}+\boldsymbol{\rho}_2)s_2]-1\}\,. \tag{A25}$$

The summation over m_1, m_2, and m_3 is easily performed one by one, starting from that over m_3. We obtain

$$H_2(s_1,s_2)=\exp\{n_i V[h_2(s_1,s_2)-h_1(s_1)-h_1(s_2)]\}\,. \tag{A26}$$

Equation (A17) is calculated with the use of Eqs. (A21), (A22), (A25), and (A26). The quantity in the curly brackets of Eq. (A17) is given by $(F_{11}-1)(F_{12}-1)(F_{21}-1)(F_{23}-1)$ neglecting the residual terms which vanish in the limit of $V\to\infty$ because of a factor $\exp(-n_i V)$ involved. Then, Eq. (A17) is found to contain a factor $H_1(s_1)H_1(s_2)H_2(s_1,s_2)=\exp[n_i V h_2(s_1,s_2)]$. We obtain

$$\bar{K}_1(\mathbf{k})=\left[\frac{1}{jG_0^R(\mathbf{k})}\right]^2\int_0^{\infty}ds_1\int_0^{\infty}ds_2\exp\left[\frac{j}{G_0^R(\mathbf{k})}(s_1+s_2)+n_i V h_2(s_1,s_2)\right]\,. \tag{A27}$$

This equation indicates that only the linked diagrams as in the case of $b=1$ in Fig. 15 contributes to $\bar{K}_1(\mathbf{k})$. We finally obtain

$$K_1(\mathbf{k})=j^{-2}\int d\boldsymbol{\rho}_1\delta(\boldsymbol{\rho}_1)\int d\boldsymbol{\rho}_2\delta(\boldsymbol{\rho}_2)\int_0^{\infty}ds_1\int_0^{\infty}ds_2\exp\left[\frac{j}{G_0^R(\mathbf{k})}(s_1+s_2)\right]O_p\left[\mathbf{k}+j\frac{\partial}{\partial\boldsymbol{\rho}_2}\right]$$
$$\times\exp\left[n_i\int d\mathbf{r}\{\exp[-jU_i(\mathbf{r}+\boldsymbol{\rho}_1)s_1-jU_i(\mathbf{r}+\boldsymbol{\rho}_2)s_2]-1\}\right]\,. \tag{A28}$$

Now we extend the calculation for $n=1$ given above to that for $K_2(\mathbf{k})$ and further to that for $K_n(\mathbf{k})$ with $n\geq 3$. Let us start with

$$K_2(\mathbf{k},\mathbf{k}')=[G_0^R(\mathbf{k})]^3\frac{1}{V}\sum_{l=0}^{\infty}\sum_{m=0}^{\infty}\sum_{n=0}^{\infty}\int d\mathbf{r}\exp[-j(\mathbf{k}-\mathbf{k}')\cdot\mathbf{r}][G_0^R(\mathbf{k})\Gamma(\mathbf{r})]^l O_p(\mathbf{k}+j\nabla)$$
$$\times[G_0^R(\mathbf{k})\Gamma(\mathbf{r})]^m O_p(\mathbf{k}+j\nabla)[G_0^R(\mathbf{k})\Gamma(\mathbf{r})]^n\,, \tag{A29}$$

which is obtained from Eq. (2.13). Equation (A29) is rewritten as

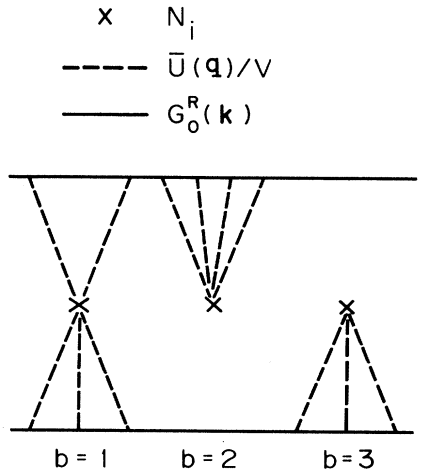

FIG. 15. Diagrams representing the terms for the electron-impurity interaction in $K_1(\mathbf{k})$, where the solid lines show $G_0^R(\mathbf{k})$, the crosses the impurity sites with each site assigned with N_i, and the dotted lines the electron-impurity interaction $\bar{U}_i(\mathbf{q})/V$ with various $\mathbf{q}$'s.

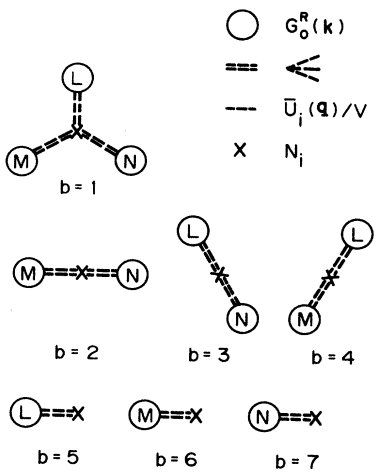

FIG. 16. Diagrams representing the terms for the electron-impurity interaction in $K_2(\mathbf{k})$, where the circles show $G_0^R(\mathbf{k})$, the crosses the impurity sites with each site assigned with N_i, and the double-dotted lines bunches of the interaction lines $\bar{U}_i(\mathbf{q})/V$ with various $\mathbf{q}$'s.

$$K_2(\mathbf{k},\mathbf{k}')=[G_0^R(\mathbf{k})]^3\sum_{l=0}^{\infty}\sum_{m=0}^{\infty}\sum_{n=0}^{\infty}\sum_{\mathbf{q}_1\mathbf{q}_2\cdots\mathbf{q}_l}\sum_{\mathbf{p}_1\mathbf{p}_2\cdots\mathbf{p}_m}\sum_{\mathbf{t}_1\mathbf{t}_2\cdots\mathbf{t}_n}$$

$$\times\Delta(\mathbf{Q}_l+\mathbf{P}_m+\mathbf{T}_n+\mathbf{k}-\mathbf{k}')O_p(\mathbf{k}-\mathbf{P}_m-\mathbf{T}_n)O_p(\mathbf{k}-\mathbf{T}_n)$$

$$\times\prod_{\lambda=1}^{l}[G_0^R(\mathbf{k})\bar{\Gamma}(\mathbf{q}_\lambda)]\prod_{\mu=1}^{m}[G_0^R(\mathbf{k})\bar{\Gamma}(\mathbf{p}_\mu)]\prod_{\nu=1}^{n}[G_0^R(\mathbf{k})\bar{\Gamma}(\mathbf{t}_\nu)]\ , \tag{A30}$$

where $\mathbf{Q}_l$, $\mathbf{P}_m$, $\mathbf{T}_n$, $\mathbf{q}_\lambda$, $\mathbf{p}_\mu$, and $\mathbf{t}_\nu$ are the wave vectors with $\mathbf{Q}_l=\sum_{\lambda=1}^{l}\mathbf{q}_\lambda$, $\mathbf{P}_m=\sum_{\mu=1}^{m}\mathbf{p}_\mu$, and $\mathbf{T}_n=\sum_{\nu=1}^{n}\mathbf{t}_\nu$. The terms of $K_2(\mathbf{k})$ which are obtained from this relation by taking an ensemble average of $K_2(\mathbf{k},\mathbf{k}')$ are schematically shown in Fig. 16. Here we have three solid lines of $G_0^R(\mathbf{k})$'s called L line, M line, and N line, which come from the factors $\prod_{\lambda=1}^{l}[G_0^R(\mathbf{k})\bar{\Gamma}(\mathbf{q}_\lambda)]$, $\prod_{\mu=1}^{m}[G_0^R(\mathbf{k})\bar{\Gamma}(\mathbf{p}_\mu)]$, and $\prod_{\nu=1}^{n}[G_0^R(\mathbf{k})\bar{\Gamma}(\mathbf{q}_\nu)]$, respectively. Those lines are represented by L, M, and N, respectively, in Fig. 16. The double-dotted lines represent bunches of the integration lines $U_i(\mathbf{q})/V$, through which the solid lines are connected to each other through the crosses representing the impurity sites assigned with N_i. For the group denoted $b=1$, each impurity site is connected to three lines L, M, and N. For the groups $b=2$, 3, and 4, each impurity site is connected to two solid lines chosen out of the three lines. For groups $b=5$, 6, and 7, the three lines are mutually independent.

As an extension of Eq. (A4) we define

$$H(\mathbf{Q}_l,\mathbf{P}_m,\mathbf{T}_n)=\Delta(\mathbf{Q}_l+\mathbf{P}_m+\mathbf{T}_n)\prod_{\lambda=1}^{l}\left[\frac{\bar{U}_i(\mathbf{q}_\lambda)}{V}\right]\prod_{\mu=1}^{m}\left[\frac{\bar{U}_i(\mathbf{p}_\mu)}{V}\right]\prod_{\nu=1}^{n}\left[\frac{\bar{U}_i(\mathbf{t}_\nu)}{V}\right]\ . \tag{A31}$$

Then the diagrams in Fig. 16 give a term of $K_2(\mathbf{k})$ analogously to Eq. (A5) as

$$S(\mathbf{L},\mathbf{M},\mathbf{N})=[G_0^R(\mathbf{k})]^{L+M+N+3}\sum_{(\mathbf{q})(\mathbf{p})(\mathbf{t})}\Delta(\mathbf{Q}+\mathbf{P}+\mathbf{T})O_p(\mathbf{k}-\mathbf{P}-\mathbf{T})O_p(\mathbf{k}-\mathbf{T})$$

$$\times\prod_{b=1}^{7}\left[(N_i)^{a_b}\prod_{c=1}^{a_b}H(\mathbf{Q}_{bl_{bc}},\mathbf{P}_{bm_{bc}},\mathbf{T}_{cn_{bc}})\right] \tag{A32}$$

under the definition of $\mathbf{L},L,\mathbf{Q}$, and some others similar to that given just below Eq. (A5). In a way analogous to the process from Eq. (A6) to (A16), we obtain

$$K_2(\mathbf{k})=[G_0^R(\mathbf{k})]^3\int d\boldsymbol{\rho}_1\delta(\boldsymbol{\rho}_1)\int d\boldsymbol{\rho}_2\delta(\boldsymbol{\rho}_2)\int d\boldsymbol{\rho}_3\delta(\boldsymbol{\rho}_3)O_p\left[\mathbf{k}+j\frac{\partial}{\partial\boldsymbol{\rho}_2}+j\frac{\partial}{\partial\boldsymbol{\rho}_3}\right]O_p\left[\mathbf{k}+j\frac{\partial}{\partial\boldsymbol{\rho}_3}\right]\bar{K}_2(\mathbf{k}) \tag{A33}$$

with

$$\bar{K}_2(\mathbf{k})=\left[\frac{1}{jG_0^R(\mathbf{k})}\right]^3\prod_{b=1}^{7}\left[\sum_{a_b=0}^{\infty}\frac{(n_i)^{a_b}}{a_b!}\int\mathcal{D}\mathbf{r}_{a_b}\right]\sum_{(l)(m)(n)}$$
$$\times\prod_{b\in L}\left[\sum_{\lambda_b=0}^{a_b-1}(-1)^{\lambda_b}\right]\prod_{b\in M}\left[\sum_{\mu_b=0}^{a_b-1}(-1)^{\mu_b}\right]\prod_{b\in N}\left[\sum_{\nu_b=0}^{a_b-1}(-1)^{\nu_b}\right]$$
$$\times\int_0^\infty ds_1\int_0^\infty ds_2\int_0^\infty ds_3\exp\left[\frac{j}{G_0^R(\mathbf{k})}(s_1+s_2+s_3)\right]$$
$$\times\left[\left[\prod_{b\in L}(F_{1b}-1)-1\right]\left[\prod_{b\in M}(F_{2b}-1)-1\right]\left[\prod_{b\in N}(F_{3b}-1)-1\right]-1\right], \tag{A34}$$

where

$$F_{1b}=\exp\left[\frac{js_1}{G_0^R(\mathbf{k})}\sum_{\sigma=1}^{a_b-\lambda_b}u_{bl_\sigma}\right]\quad(b\in L),$$
$$F_{2b}=\exp\left[\frac{js_2}{G_0^R(\mathbf{k})}\sum_{\sigma=1}^{a_b-\mu_b}v_{bm_\sigma}\right]\quad(b\in M), \tag{A35}$$
$$F_{3b}=\exp\left[\frac{js_3}{G_0^R(\mathbf{k})}\sum_{\sigma=1}^{a_b-\nu_b}w_{bn_\sigma}\right]\quad(b\in N),$$

with $u_{bc}=G_0^R(\mathbf{k})U_i(\mathbf{r}_{bc}+\boldsymbol{\rho}_1)$, $v_{bc}=G_0^R(\mathbf{k})U_i(\mathbf{r}_{bc}+\boldsymbol{\rho}_2)$, and $w_{bc}=G_0^R(\mathbf{k})U_i(\mathbf{r}_{bc}+\boldsymbol{\rho}_3)$; (l), (m), and (n) in Eq. (A34) refer to l_σ, m_σ, and n_σ, respectively, in Eq. (A35). In Eqs. (A34) and (A35), $b\in L$ (M or N) means that b runs over the diagrams in Fig. 16, containing L (M or N) line, i.e., $b=1,3,4,5$ for $b\in L$, $b=1,2,4,6$ for $b\in M$, and $b=1,2,3,7$ for $b\in N$. Thus, referring to Fig. 16, the rule for obtaining Eq. (A34) is evident and the extension to a general case of $K_n(\mathbf{k})$ is straightforward.

Equation (A34) is given in terms of H_1 as in Eq. (A19), H_2 as in Eq. (A20), and

$$H_3(s_1,s_2,s_3)=\sum_{a_1=0}^{\infty}\frac{(n_i)^{a_1}}{a_1!}\sum_{(l)(m)(n)}\sum_{\lambda_1=0}^{a_1-1}\sum_{\mu_1=0}^{a_1-1}\sum_{\nu_1=0}^{a_1-1}\int\mathcal{D}\mathbf{r}_{a_1}[F_{11}(a_1-\lambda_1)-1][F_{21}(a_1-\mu_1)-1][F_{31}(a_1-\nu_1)-1], \tag{A36}$$

where F_{1b}, F_{2b}, and F_{3b} are expressed as functions of $a_b-\lambda_b$, $a_b-\mu_b$, and $a_b-\nu_b$, respectively, noting Eq. (A7).

Analogously to the case of H_2, we find

$$H_3(s_1,s_2,s_3)=\sum_{a_1=0}^{\infty}(n_iV)^{a_1}\prod_{b=1}^{7}\left[\sum_{m_b=0}^{a_1}\frac{1}{m_b!}\right]\frac{1}{\left[a_1-\sum_{b=1}^{7}m_b\right]!}$$
$$\times\zeta\left[a_1-\sum_{b\in L}m_b\right]\zeta\left[a_1-\sum_{b\in M}m_b\right]\zeta\left[a_1-\sum_{b\in N}m_b\right]$$
$$\times[h_3(s_1,s_2,s_3)+1]^{m_1}[-h_2(s_2,s_3)-1]^{m_2}[-h_2(s_3,s_1)-1]^{m_3}[-h_2(s_1,s_2)-1]^{m_4}$$
$$\times[h_1(s_1)+1]^{m_5}[h_1(s_2)+1]^{m_6}[h_1(s_3)+1]^{m_7}, \tag{A37}$$

where $\zeta(x)=1$ and $x\geq 0$ and $\zeta(x)=0$ otherwise, and

$$h_3(s_1,s_2,s_3)=\frac{1}{V}\int d\mathbf{r}\left[\exp\left[-j\sum_{l=1}^{3}U_i(\mathbf{r}+\boldsymbol{\rho}_l)s_l\right]-1\right]. \tag{A38}$$

Equation (A37) becomes

$$H_3(s_1,s_2,s_3)=\exp\{n_iV[h_3(s_1,s_2,s_3)-h_2(s_2,s_3)-h_2(s_3,s_1)-h_2(s_1,s_2)-h_1(s_1)-h_1(s_2)-h_1(s_3)]\}. \tag{A39}$$

Now we neglect the terms in Eq. (A34) which vanish in the limit of $V\to\infty$ due to the factor $\exp(-n_iV)$ involved. Then the quantity in the large square brackets of Eq. (A34) is given as the product of four $(F_{1b}-1)$'s with $b\in L$ times the product of four $(F_{2b}-1)$'s with $b\in M$ times the product of four $(F_{3b}-1)$'s with $b\in N$. This situation is similar for a general case of $\bar{K}_n(\mathbf{k})$; we construct the product of $(F_{ib}-1)$ with all b's allowable for a given solid line i

$(=1,2,\ldots,n)$ and then obtain the product of all those products. Equation (A34) is found to contain the product of the factors, i.e.,

$$H_3(s_1,s_2,s_3)H_2(s_2,s_3)H_2(s_3,s_1)H_2(s_1,s_2)H_1(s_1)H_1(s_2)H_1(s_3)\ . \tag{A40}$$

Each factor comes from one of the diagrams in Fig. 16 and the factors are placed from the left to the right in the increasing order of b for the corresponding diagrams. Note that we have s_1, s_2, and s_3 correspondingly to the L, M, and N lines, respectively. From Eq. (A40) we obtain

$$\bar{K}_2(\mathbf{k})=\left[\frac{1}{jG_0^R(\mathbf{k})}\right]^3\int_0^\infty ds_1\int_0^\infty ds_2\int_0^\infty ds_3\exp\left[\frac{j}{G_0^R(\mathbf{k})}(s_1+s_2+s_3)+n_iVh_3(s_1,s_2,s_3)\right]\ . \tag{A41}$$

As a result we have

$$K_2(\mathbf{k})=j^{-3}\int_0^\infty ds_1\int_0^\infty ds_2\int_0^\infty ds_3\exp\left[\frac{j}{G_0^R(\mathbf{k})}(s_1+s_2+s_3)\right]\int d\boldsymbol{\rho}_1\delta(\boldsymbol{\rho}_1)\int d\boldsymbol{\rho}_2\delta(\boldsymbol{\rho}_2)\int d\boldsymbol{\rho}_3\delta(\boldsymbol{\rho}_3)$$

$$\times O_p\left[\mathbf{k}+j\frac{\partial}{\partial\boldsymbol{\rho}_2}+j\frac{\partial}{\partial\boldsymbol{\rho}_3}\right]O_p\left[\mathbf{k}+j\frac{\partial}{\partial\boldsymbol{\rho}_3}\right]\exp\left\{n_i\int d\mathbf{r}\left[\exp\left[-j\sum_{l=1}^{3}U_i(\mathbf{r}+\boldsymbol{\rho}_l)\right]-1\right]\right\}\ . \tag{A42}$$

On the basis of the discussions given for $K_1(\mathbf{k})$ and $K_2(\mathbf{k})$, we can obtain $K_n(\mathbf{k})$ easily. As an extension of Eq. (A33), we start with

$$K_n(\mathbf{k})=[G_0^R(\mathbf{k})]^{n+1}\int d\boldsymbol{\rho}_1\delta(\boldsymbol{\rho}_1)\prod_{l=2}^{n+1}\left[\int d\boldsymbol{\rho}_l\delta(\boldsymbol{\rho}_l)\right]\prod_{l=2}^{n+1}\left[O_p\left[\mathbf{k}+j\sum_{m=l}^{n+1}\frac{\partial}{\partial\boldsymbol{\rho}_m}\right]\right]\bar{K}_n(\mathbf{k})\ . \tag{A43}$$

In the diagrams for $\bar{K}_n(\mathbf{k})$ as in Figs. 15 and 16, there are $n+1$ solid lines, for which we consider all possible combinations of various number of the solid lines connected to one impurity site by the interaction lines. For the moment we do not consider the number of the interaction lines, as in Fig. 16. Then we have $\binom{n+1}{m}$ ways of connecting m solid lines (including $m=1$ as in the case of $b=5$, 6, and 7 in Fig. 16). The number of all those ways, i.e., the groups b's, is

$$\sum_{m=1}^{n+1}\binom{n+1}{m}=2^{n+1}-1\equiv b_{\max}\ . \tag{A44}$$

On the other hand, we have $\binom{n}{m}$ ways of finding m solid lines connected to a given solid line, so that the number of all those ways is

$$\sum_{m=0}^{n}\binom{n}{m}=2^n\ ,$$

including also the case where the given solid line is unconnected. In place of four in Eq. (A34), we have 2^n factors $\sum_{\lambda_{lb}}(-1)^{\lambda_{lb}}(F_{lb}-1)$ for a given solid line l $(1\le l\le n+1)$ and for such various groups b $(1\le b\le b_{\max})$ as contain the solid line l. Neglecting the terms which vanish in the limit of $V\to\infty$ due to the factor $\exp(-n_iV)$ involved, we obtain

$$\bar{K}_n(\mathbf{k})=\left[\frac{1}{jG_0^R(\mathbf{k})}\right]^{n+1}\prod_{b=1}^{b_{\max}}\left[\sum_{a_b=0}^{\infty}\frac{(n_i)^{a_b}}{a_b!}\int\mathcal{D}\mathbf{r}_{a_b}\right]\prod_{l=1}^{n+1}\left[\sum_{(c)}\int_0^\infty ds_l\right]\left[\mathcal{P}_{(n+1)2^n}\sum_{\lambda_{lb}}(-1)^{\lambda_{lb}}(F_{lb}-1)\right]\ , \tag{A45}$$

where $\mathcal{P}_m$ represents the product of m factors and we define

$$F_{lb}=\exp\left[\frac{js_l}{G_0^R(\mathbf{k})}\sum_{\sigma=1}^{a_b-\lambda_{lb}}u^l_{bc_\sigma}\right] \tag{A46}$$

with $u^l_{bc}=G_0^R(\mathbf{k})U_i(\mathbf{r}_{bc}+\boldsymbol{\rho}_l)$; (c) in Eq. (A45) refers to c_σ in Eq. (4.18) meaning all possible choices of c_σ's. Then $\bar{K}_n(\mathbf{k})$ is given in terms of the factors

$$H_m(s_{l_1},s_{l_2},\ldots,s_{l_m})=\sum_{a_b=0}^{\infty}\frac{(n_i)^{a_b}}{a_b!}\prod_{l=1}^{n+1}\left[\sum_{(c)}\sum_{\lambda_{lb}}\right]\int\mathcal{D}\mathbf{r}_{a_b}\left[\mathcal{P}_m\sum_{\lambda_{lb}}(-1)^{\lambda_{lb}}(F_{lb}-1)\right]\ , \tag{A47}$$

where b denotes the group of the connected m solid lines $l_1,l_2,\ldots,l_m$ picked out of the $n+1$ solid lines. Defining

$$h_m(s_{l_1},s_{l_2},\ldots,s_{l_m})=\frac{1}{V}\int d\mathbf{r}\left[\exp\left[-j\sum_{\sigma=1}^{m}U_i(\mathbf{r}+\boldsymbol{\rho}_{l\sigma})s_{l\sigma}\right]-1\right], \tag{A48}$$

we find

$$H_m(s_{l_1},s_{l_2},\ldots,s_{l_m})=\exp\left\{n_iV\left[\sum_{l=1}^{m}(-1)^{m-l}\begin{bmatrix}m\\l\end{bmatrix}h_l\right]\right\}, \tag{A49}$$

where h_l is a symbolic expression for the function defined by Eq. (A48); $\binom{m}{l}h_l$ means simply that the number of h_l's is $\binom{m}{l}$ with all h_l's being different.

As in Eq. (A40), $\bar{K}_n(\mathbf{k})$ contains the product of the factors as

$$\prod_{m=1}^{n+1}(H_m)^{\binom{n+1}{m}}, \tag{A50}$$

which is also a symbolical expression meaning simply that the number of H_m's for a given m is $\binom{n+1}{m}$ with all H_m's being different. Use of Eq. (A49) in Eq. (A50) gives a form of $\exp(n_iVS)$ with

$$S=\sum_{m=1}^{n+1}\begin{bmatrix}n+1\\m\end{bmatrix}\sum_{l=1}^{m}(-1)^{m-l}\begin{bmatrix}m\\l\end{bmatrix}h_l$$

$$=h_{n+1}\,. \tag{A51}$$

As a result we obtain

$$\bar{K}_n(\mathbf{k})=\left[\frac{1}{jG_0^R(\mathbf{k})}\right]^{n+1}\int_0^\infty ds_1\int_0^\infty ds_2\cdots\int_0^\infty ds_{n+1}\exp\left[\frac{j}{G_0^R(\mathbf{k})}(s_1+s_2+\cdots+s_{n+1})\right.$$

$$\left.+n_iVh_{n+1}(s_1,s_2,\ldots,s_{n+1})\right], \tag{A52}$$

from which $K_n(\mathbf{k})$ is obtained. With a slight change of notation we have Eq. (2.17).

APPENDIX B: APPROXIMATIONS YIELDING TRACTABLE $G^R(\mathbf{k})$

We put expression (2.14) under Eqs. (2.16) and (2.17) for the one-particle Green's function into a more tractable but approximate form. Let us restrict the discussion hereafter to the case where $U_i(\mathbf{r})$ is spherically symmetric, so that we write $U_i(\mathbf{r})$ as $U_i(r)$. Then we replace O_p in Eq. (2.17) approximately with

$$O_k=-\frac{\hbar^2}{2m_c}\left|\sum_l\nabla_l\right|^2+j\frac{\hbar^2}{m_F}\mathbf{k}\cdot\sum_l\nabla_l\,, \tag{B1}$$

where $\mathbf{k}$ is in the new coordinate system; here we have considered an average over all the directions. Strictly, Eq. (B1) is useful for $K_1(\mathbf{k})$ and for some factors in $K_n(\mathbf{k})$. Approximate validity of using Eq. (B1) is found from a numerical result for anisotropic mass.

Now we pick up typical terms in $K_n(\mathbf{k})$ by defining

$$P_m^n(\mathbf{r})=-j\frac{\hbar^2}{2m_c}|\nabla U_i(r)|^2\left[\sum_{l=m}^{n}s_l\right]^2$$

$$+\left[\frac{\hbar^2}{2m_c}\nabla^2U_i(r)-j\frac{\hbar^2}{m_F}\mathbf{k}\cdot\nabla U_i(r)\right]\sum_{l=m}^{n}s_l\,, \tag{B2}$$

the operator $\mathcal{J}_n(\mathbf{r})$ upon a function $F(\mathbf{r})$ as

$$\mathcal{J}_nF(\mathbf{r})=n_i\int d\mathbf{r}\exp\left[-jU_i(r)\sum_{l=0}^{n}s_l\right]F(\mathbf{r})\,, \tag{B3}$$

and S_n by

$$K_n(\mathbf{k})=j^{-1}\prod_{l=0}^{n}\left[\int_0^\infty ds_l\exp\left[\frac{j}{G_i^R(\mathbf{k})}s_l\right]\right]\exp\left\{n_i\int d\mathbf{r}\left[\exp\left[-j\sum_{m=0}^{n}U_i(r)s_m\right]-1\right]\right\}S_n\,. \tag{B4}$$

The problem is now to examine S_n by noting the relation

$$\int d\mathbf{r} \exp\left[-j\sum_l U_i(r)s_l\right]\frac{\partial}{\partial \mathbf{r}}\exp[-jU_i(r)s_m]=0 . \quad \text{(B5)}$$

First we have $S_0=1$ and

$$S_1=\mathcal{I}_1(\mathbf{r})P_1(\mathbf{r}) . \quad \text{(B6)}$$

Next we have

$$S_2=[\mathcal{I}_2(\mathbf{r})P_2^2(\mathbf{r})][\mathcal{I}_2(\mathbf{r})P_1^2(\mathbf{r})] + \mathcal{I}_2(\mathbf{r})P_2^2(\mathbf{r})P_1^2(\mathbf{r})+\cdots , \quad \text{(B7)}$$

where the ellipsis represents residual terms.

For a typical form of $U_i(r)$ such as the Thomas-Fermi screened Coulomb potential, the first term and the second term in Eq. (B7) are finite and infinite, respectively. The infiniteness of the second term is related to the divergence of $U_i(r)$ at $r\to 0$. On the other hand, the contribution of $U_i(r)$ at large values of r is larger to the first term than to the second term. The residual terms in Eq. (B7) such as

$$\left[\mathcal{I}_n(\mathbf{r})\frac{\hbar^2}{2m_c}|\nabla U_i(r)|^2 s_1 s_2\right]^2$$

are intermediate between the first and the second terms. The situation in $K_2(\mathbf{k})$ is similar to that in $K_n(\mathbf{k})$ with $n\geq 3$, so that we pick up only the terms similar to the first and the second terms in Eq. (B7). We obtain

$$S_n=\sum_{\nu=1}^{n}\prod_{\lambda=1}^{\nu}\mathcal{I}_n(\mathbf{r}_\lambda)\sum_{(m_\mu)}\prod_{\mu=1}^{\nu}[P(\mathbf{r}_\mu)]^{m_\mu}\Delta\left[\sum_{\mu=1}^{\nu}m_\mu-n\right] , \quad \text{(B8)}$$

where $[P(\mathbf{r}_\mu)]^{m_\mu}$ is a symbolic expression for the product of m_μ factors of $P_m^n(\mathbf{r}_\mu)$ with m picked out from the integers between 1 and n without repeated choices of the same number, and $\sum_{(m_\mu)}$ means the summation over all possible ways; we define $\Delta(x)=1$ for $x=0$ and $\Delta(x)=0$ otherwise.

In order to proceed further, we define new variables $t_m=\sum_{l=m}^{n}s_l$ for all integers m in the range $0\leq m\leq n$. Then $K_n(\mathbf{k})$ is given in terms of t_m's. We obtain (using t in place of t_0)

$$K_n(\mathbf{k})=\frac{1}{j}\int_0^\infty dt\exp\left[\frac{j}{G_1^R(\mathbf{k})}t + n_i\int d\mathbf{r}\{\exp[-jU_i(r)t] -1\}\right]T_n(t) , \quad \text{(B9)}$$

where

$$T_n(t_0)=\int_0^t dt_1\int_0^{t_1}dt_2\cdots\int_0^{t_{n-1}}dt_n S_n . \quad \text{(B10)}$$

Here, S_n is given in terms of the integration operator

$$\mathcal{I}_n(\mathbf{r})=\mathcal{I}(\mathbf{r})=n_i\int d\mathbf{r}\exp[-jU_i(r)t] \quad \text{(B11)}$$

and

$$P_m^n(\mathbf{r})=-j\frac{\hbar^2}{2m_c}|\nabla U_i(r)|^2 t_m^2 + \left[\frac{\hbar^2}{2m_c}\nabla^2 U_i(r)-j\frac{\hbar^2}{m_F}\mathbf{k}\cdot\nabla U_i(r)\right]t_m . \quad \text{(B12)}$$

From Eq. (B8) we obtain

$$T_n(t)=\sum_{\nu=1}^{n}\prod_{\lambda=1}^{\nu}\mathcal{I}(\mathbf{r}_\lambda)R_n(\mathbf{r}_1,\mathbf{r}_2,\ldots,\mathbf{r}_\nu;t) , \quad \text{(B13)}$$

where

$$R_n(\mathbf{r}_1,\mathbf{r}_2,\ldots,\mathbf{r}_\nu;t)=\int_0^t dt_1\int_0^{t_1}dt_2\cdots\int_0^{t_{n-1}}dt_n\sum_{(m_\mu)}\prod_{\mu=1}^{\nu}[P_{m_\mu}^n(\mathbf{r}_\mu)]^{m_\mu}\Delta\left[\sum_{\mu=1}^{n}m_\mu-n\right] . \quad \text{(B14)}$$

This equation is rewritten as

$$R_n(\mathbf{r}_1,\mathbf{r}_2,\ldots,\mathbf{r}_\nu;t)=\int_0^t dt_1\int_0^{t_1}dt_2\cdots\int_0^{t_{n-1}}dt_n\prod_{m=1}^{n}\left[\sum_{\mu=1}^{\nu}P_m^n(\mathbf{r}_\mu)\right] . \quad \text{(B15)}$$

With the use of Eq. (B12) we find

$$R_n(\mathbf{r}_1,\mathbf{r}_2,\ldots,\mathbf{r}_\nu;t)=\frac{1}{n!}\left[\sum_{\mu=1}^{\nu}B(\mathbf{r}_\mu,t)\right]^n , \quad \text{(B16)}$$

where we define

$$B(\mathbf{r}_\mu,t)=-j\frac{\hbar^2}{2m_C}|\nabla_\mu U_i(r_\mu)|^2\frac{t^3}{3} + \left[\frac{\hbar^2}{2m_c}\nabla_\mu^2 U_i(r_\mu)-j\frac{\hbar^2}{m_F}\mathbf{k}\cdot\nabla_\mu U_i(r_\mu)\right]\frac{t^2}{2} . \quad \text{(B17)}$$

With the use of Eqs. (B1), (B9), and (B12) we obtain

$$G^R(\mathbf{k})=\frac{1}{j}\int_0^\infty dt\exp\left[\frac{j}{G_1^R(\mathbf{k})}t + n_i\int d\mathbf{r}\{\exp[-jU_i(r)t] -1\}\right]T(t) , \quad \text{(B18)}$$

where

$$T(t)=\sum_{n=0}^{\infty}\frac{1}{n!}\sum_{\nu=1}^{n}\left[\prod_{\lambda=1}^{\nu}\mathcal{I}(\mathbf{r}_\lambda)\right]\left[\sum_{\mu=1}^{\nu}B_\mu\right]^n \quad \text{(B19)}$$

with the abbreviation $B_\mu = B(\mathbf{r}_\mu, t)$; the term for $n=0$ in the equation is unity.

The summation in Eq. (B19) is performed by rewriting the equation as

$$T(t)=\sum_{n=0}^{\infty}\sum_{\nu=1}^{n}\sum_{(m_\mu)}\frac{A^{m_1}}{m_1!}\prod_{\mu=2}^{\nu}\left[\frac{1}{m_\mu!}\mathcal{J}(\mathbf{r}_\mu)(B_\mu)^{m_\mu}\right]\times\Delta\left[\sum_{\lambda=1}^{\nu}m_\lambda-n\right], \tag{B20}$$

where $A=\mathcal{J}(\mathbf{r}_1)B_1=\mathcal{J}(\mathbf{r})B(\mathbf{r},t)$. We first consider the case of $m_1=n$ and m_μ $(\mu\geq 2)=0$, obtaining the first partial sum in $T(t)$:

$$\sum_{n=0}^{\infty}\frac{A^n}{n!}=\exp A\ . \tag{B21}$$

For the residual part in $T(t)$, we consider the case of $m_1=n-m$ (≥ 0), $m_2=m$ (≥ 2), and m_μ $(\mu\geq 3)=0$, obtaining the second partial sum

$$\mathcal{J}(\mathbf{r}_2)\sum_{n=2}^{\infty}\sum_{m=2}^{n}\frac{A^{n-m}(B_2)^m}{(n-m)!m!}=\exp A\,\mathcal{J}(\mathbf{r})[\exp B(\mathbf{r},t)-B(\mathbf{r},t)-1]\ . \tag{B22}$$

For the rest of the sum we consider the case of $m_1=n-m_2-m_3$ (≥ 0), $m_2\geq 2$, $m_3\geq m_2$, and m_μ $(\mu\geq 4)=0$, obtaining the third partial sum

$$\mathcal{J}(\mathbf{r}_2)\mathcal{J}(\mathbf{r}_3)\sum_{n=4}^{\infty}\sum_{m_2=2}^{n}\sum_{m_3=m_2}^{n}\frac{A^{n-m_2-m_3}(B_2)^{m_2}(B_3)^{m_3}}{(n-m_2-m_3)!m_2!m_3!}$$

$$=\exp A\,\mathcal{J}(\mathbf{r}_2)\mathcal{J}(\mathbf{r}_3)\sum_{m_2=2}^{\infty}\sum_{m_3=m_2}^{\infty}\frac{(B_2)^{m_2}(B_3)^{m_3}}{m_2!m_3!}$$

$$=\frac{1}{2!}\exp A\,\mathcal{J}(\mathbf{r}_2)\mathcal{J}(\mathbf{r}_3)\left[\sum_{m_2=2}^{\infty}\frac{B_2^{m_2}}{m_2!}\left[\sum_{m_3=2}^{\infty}\frac{B_3^{m_3}}{m_3!}+\frac{B_2^{m_2}}{m_2!}\right]\right]$$

$$=\frac{1}{2!}\exp A\{\mathcal{J}(\mathbf{r})[\exp B(\mathbf{r},t)-B(\mathbf{r},t)-1]\}^2\ . \tag{B23}$$

The last step is reached by neglecting the second term in the large parentheses in the second to last step. This is a crude approximation adopted on the basis that in the large parentheses the first term is equal to or larger in magnitude than the second term. In a similar way we obtain the $m+1$th partial sum for $m\geq 3$ as

$$\frac{1}{m!}\exp A\{\mathcal{J}(\mathbf{r})[\exp B(\mathbf{r},t)-B(\mathbf{r},t)-1]\}^m \tag{B24}$$

using the approximation as in Eq. (B23). The sum of the terms in Eqs. (B21)–(B24) gives

$$T(t)=\exp\{A+\mathcal{J}(\mathbf{r})[\exp B(\mathbf{r},t)-B(\mathbf{r},t)-1]\}\ . \tag{B25}$$

The final form of $G^R(\mathbf{k})$ is

$$G^R(\mathbf{k})=\frac{1}{j}\int_0^\infty dt\,\exp\left[\frac{j}{G_1^R(\mathbf{k})}t+n_i\int d\mathbf{r}\{\exp[-jU_i(r)t+B(\mathbf{r},t)]-1\}\right], \tag{B26}$$

where

$$B(\mathbf{r},t)=-j\frac{t^3}{3}\frac{\hbar^2}{2m_c}|\nabla U_i(r)|^2+\frac{t^2}{2}\left[\frac{\hbar^2}{2m_C}\nabla^2U_i(r)-j\frac{\hbar^2}{m_F}\mathbf{k}\cdot\nabla U_i(r)\right]. \tag{B27}$$

[1] E. Conwell and V. L. Weisskopf, Phys. Rev. **69**, 258 (1946).
[2] H. Brooks, Adv. Electron. Electron Phys. **7**, 85 (1955).
[3] R. B. Dingle, Philos. Mag. **46**, 831 (1955).
[4] P. Csavisky, Phys. Rev. **126**, 1436 (1962); **131**, 2033 (1963); **135**, AB3 (1964).
[5] Yu. V. Gulyaev, Fiz. Tverd. Tela **1**, 422 (1959) [Sov. Phys.—Solid State **1**, 381 (1959)].
[6] D. Hawarth and E. H. Sondheimer, Proc. Phys. Soc. London, Sect. A **219**, 53 (1953).
[7] H. Ehrenreich, J. Appl. Phys. **32**, 2155 (1961).
[8] D. L. Rode, in *Semiconductors and Semimetals*, edited by R. K. Willardson and A. C. Beer (Academic, New York, 1975), Vol. 10, Chap. 1.
[9] J. D. Wiley, Ref. 8, Chap. 2.
[10] M. J. Katz, Phys. Rev. A **140**, 1323 (1965).
[11] T. Saso and T. Kasuya, J. Phys. Soc. Jpn. **48**, 1566 (1980).

[12]T. Saso and T. Kasuya, J. Phys. Soc. Jpn. **49**, 578 (1980).
[13]T. Saso and T. Kasuya, J. Phys. Soc. Jpn. **49**, Suppl. A383 (1980).
[14]R. H. Parmenter, Phys. Rev. **97**, 587 (1955); **104**, 22 (1956).
[15]M. Lax, Rev. Mod. Phys. **23**, 287 (1951); Phys. Rev. **85**, 621 (1952).
[16]S. F. Edwards, Philos. Mag. **6**, 617 (1961).
[17]E. O. Kane, Phys. Rev. **131**, 79 (1963).
[18]G. Lasher and F. Stern, Phys. Rev. **133**, A553 (1964).
[19]D. F. Nelson, M. Gershenzon, A. Ashkin, L. A. D'Asaro, and J. C. Sarace, Appl. Phys. Lett. **2**, 182 (1963).
[20]B. I. Halperin and M. Lax, Phys. Rev. **148**, 722 (1966).
[21]V. Sa-yakanit and H. R. Glyde, Phys. Rev. B **22**, 6222 (1980).
[22]M. Takeshima, Phys. Rev. B **27**, 2387 (1983).
[23]M. Takeshima, Phys. Rev. B **30**, 4540 (1984).
[24]V. L. Bonch-Bruevich, in *Semiconductors and Semimetals,* edited by R. K. Willardson and A. C. Beer (Academic, New York, 1966), Vol. 1, Chap. 4.
[25]M. Takeshima, Phys. Rev. B **25**, 5390 (1982).
[26]M. Takeshima, Phys. Rev. B **27**, 7524 (1983).
[27]A. H. Titkov, G. H. Iluridthe, I. F. Mironov, and B. A. Cheban, Phys. Technol. Semicond. B **20**, 25 (1986).
[28]M. Takeshima, Phys. Rev. B **36**, 1186 (1987).
[29]M. Takeshima, Phys. Rev. B **37**, 2707 (1988).
[30]M. Takeshima, Phys. Rev. B **23**, 6625 (1981).
[31]S. Doniach and E. H. Sondheimer, *Green's Function for Solid State Physicists* (Benjamin, London, 1974).
[32]W. Lochmann, Phys. Status Solidi A **42**, 181 (1977).
[33]M. Takeshima, J. Phys. Soc. Jpn. **56**, 4003 (1987).
[34]S. T. Pantelides and C. T. Sah, Phys. Rev. B **10**, 621 (1974); **10**, 638 (1974).
[35]W. Kohn, in *Solid State Physics,* edited by F. Seitz and D. Turnbull (Academic, New York, 1957), Vol. 5, p. 257.
[36]M. Newberger, *III-V Semiconducting Compounds* (IFI/Plenum, New York, 1971).
[37]N. F. Mott, Can. J. Phys. **3**, 1356 (1956).
[38]G. D. Mahan and J. W. Conley, Appl. Phys. Lett. **11**, 29 (1967).
[39]Y. Furukawa, J. Phys. Soc. Jpn. **17**, 630 (1962). The resistivities are calculated from mobility data.
[40]The present calculation gives somewhat larger resistivities than in Refs. 28 and 29 because of the use of the revised method of the numerical calculation.
[41]C. Yamanouchi, K. Mizuguchi, and W. Sasaki, J. Phys. Soc. Jpn. **22**, 859 (1967).
[42]M. Takeshima, Phys. Rev. B **32**, 8066 (1985).
[43]J. S. Blakemore, *Semiconductor Statistics* (Pergamon, London, 1962), Chap. 2.
[44]H. Fritzsche, J. Phys. Chem. Solids **6**, 69 (1958).
[45]P. F. Newman and D. F. Holcomb, Phys. Rev. B **28**, 638 (1983).